Molecular Design of Heme Enzyme Active Site

Isao Hara

DOCTOR OF PHILOSOPHY

Department of Structural Molecular Science
School of Mathematical and Physical Science
The Graduate University for Advanced Studies

2001

CONTENTS

CONTENTS

PART I GENERAL INTRODUCTION 1

PART II ROLES OF AN ELECTRON-RICH TRYPTOPHAN RESIDUE IN THE HEME ACTIVE SITE 6

Chapter 1.
Effects of an Electron-Rich Tryptophan Residue on the Catalysis. 7

Chapter 2.
Regulation of Substrate Binding in the Heme Enzyme Active Site. 30

PART III EFFECTS OF A PHENOLATE AXIAL LIGAND ON THE HEME ENVIRONMENTAL STRUCTURE 47

PART IV SUMMARY AND CONCLUSIONS 68

ACKNOWLEDGMENT 71

LIST OF PUBLICATIONS 72

PART I

GENERAL INTRODUCTION

The common feature of all heme proteins is that their active sites contain very similar protoporphyrin IX prosthetic groups (Figure 1). Two hydrogen atoms attached to pyrrole nitrogens have displaced by the iron for ferriprotoporphyrin IX. Therefore, the net charge on the heme with four-coordinate iron(III) is +1. Proteins containing heme prosthetic groups play such diverse roles as reversibly binding dioxygen for transport and storage (hemoglobin and myoglobin), transfer electrons one at a time in membranous respiratory chains (cytochromes), utilizing peroxides (catalases and peroxidases), and acting as terminal component in multienzyme systems involved in hydroxylations (cytochrome P-450) (Table 1).(1)

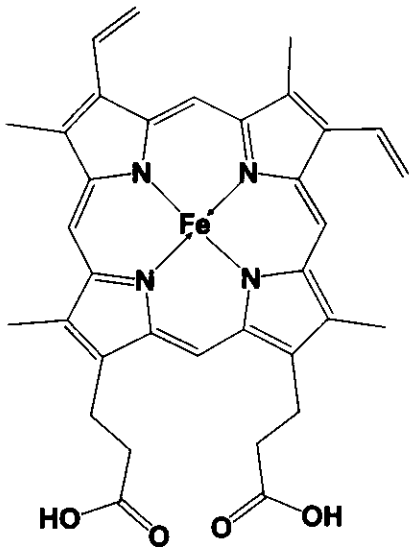

Figure 1. Structure of ferriprotoporphyrin IX.

Table 1. Biological functions of heme proteins.(2)

Biological function	Heme Protein
O_2 transportation	Hemoglobin, Myoglobin
Respiratory chain	Cytochrome oxidase
Monooxygenation	Cytochrome P-450
H_2O_2 activation	Peroxidase
H_2O_2 dismutation	Catalase
NO synthesis	NO synthase
NO reduction	P-450nor
Heme metabolism	Heme oxygenase

To elucidate structure-function relationship of heme enzymes, sperm whale myoglobin (Mb) has been employed as a building block to reconstruct essential elements of heme enzymes (Figure 2A).(3-5) On the basis of distance between distal histidine and heme iron of Mb compared with that of peroxidase, Ozaki et al. have constructed F43H/H64L Mb in which the distal histidine has been optimally relocated to serve as a general acid-base catalyst (Figure 2B).(6) By using F43H/H64L Mb, common reactive intermediate of heme enzyme, a ferryl porphyrin radical cation (compound I, $O=Fe^{IV}$porphyrin$^{\bullet+}$) was successfully prepared. This result indicates that (a) His-64 in wild type Mb destabilizes a ferryl porphyrin radical cation and decreases the catalytic activity, and (b) the replacement of Phe-43 with a histidine residue, a general-acid base catalyst, accelerates the activation of hydrogen peroxide.

Although, the F43H/H64L Mb exhibits up to 300-fold better styrene epoxidation activity with respect to the wild type, the hydroxylation is limited to the reaction at the benzylic carbon where the C–H bond is weaker than that in aliphatic or aromatic compounds. On the contrary, cytochromes P-450 (P-450) catalyze the hydroxylation of a wide variety of substrates including hydrocarbons and polycyclic aromatic molecules.(7,8) Comparison of the active site structures reveals that the variance in reactivity of Mb and P-450 could arise from differences in the active site structure and the arrangement of functional amino acid residues (Figure 2C).(9)

Natural heme proteins with protein-derived oxygen donor ligands are relatively rare. The best known natural examples are the tyrosinate ligated heme containing catalases which are responsible for the dismutation of hydrogen peroxide.(10-12) Since it is also known that the histidine-ligated heme containing peroxidase are very efficient in activation of H_2O_2,(13-16) and interestingly F43H/H64L Mb exhibits catalase activity,(17) the reasons for evolutionary selection of the tyrosinate proximal ligand for catalase remain unclear.

In this thesis, Mb mutants utilize to reconstruct essential elements of heme enzyme, and its oxidation activities and structures are examined.

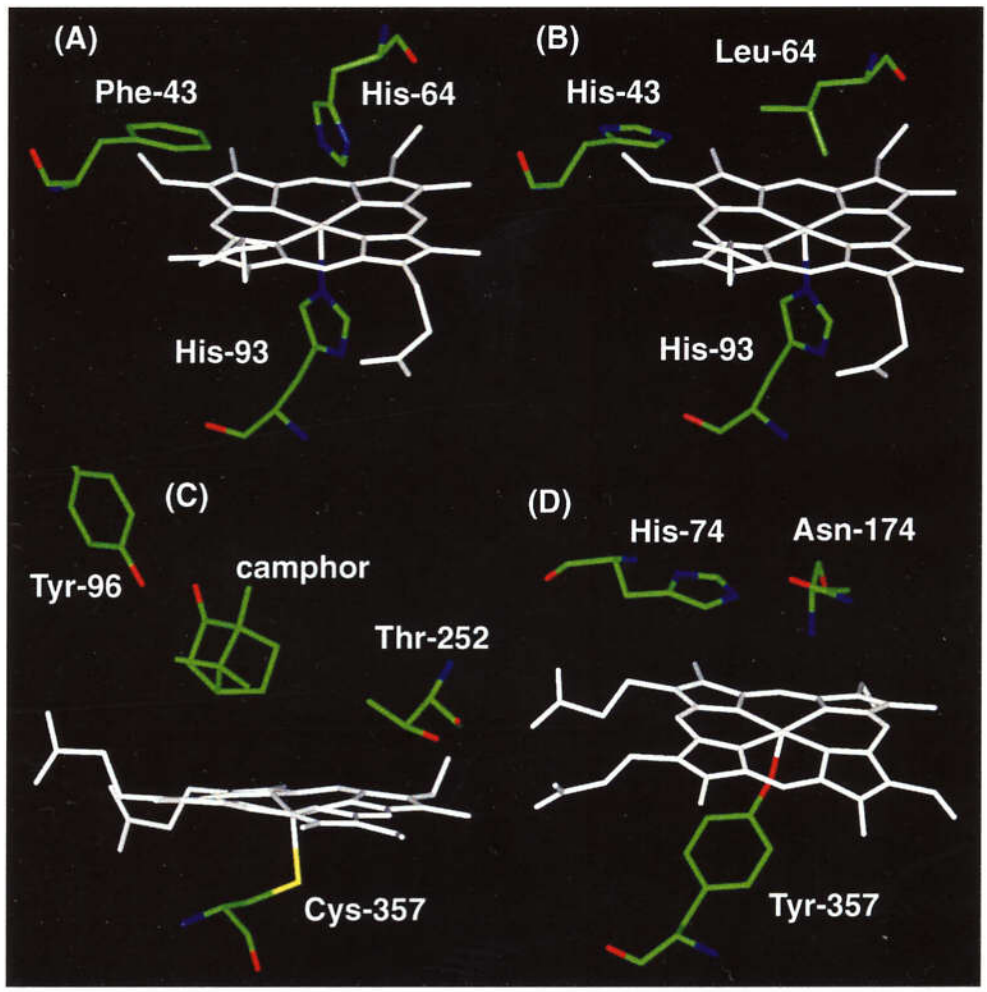

Figure 2. Active site structures of (A) sperm whale Mb, (B) F43H/H64L Mb, (C) cytochrome P-450cam, and (D) bovine liver catalase. Heme, axial ligand, and some selected distal residues are presented in the figure.

REFERENCE

1. Walsh, C. (1979) Enzymatic Reaction Mechanisms, Chapter 15, W. H. Freeman and Company, San Francisco
2. Ochiai, E. (1977) Bioinorganic Chemistry: An Introduction, Allyn and Bacon, Inc., Boston
3. Ozaki, S., Matsui, T., Roach, M. P., and Watanabe, Y. (2000) Coord. Chem. Review 198, 39-59

4. Wan, L., Twitchett, M. B., Eltis, L. D., Mauk, A. G., and Smith, M. (1998) Proc. Natl. Acad. Sci. U.S.A. 95, 12825-12831

5. Wittenberg, J., and Wittenberg, B. (1990) Annu. Rev. Biophys. Biophys. Chem. 19, 217-41

6. Ozaki, S., Matsui, T., and Watanabe, Y. (1997) J. Am. Chem. Soc. 119, 6666-6667

7. Ortiz de Montellano, P. R. (1995) in Cytochrome P450 (2nd Ed) (Ortiz de Montellano, P. R., ed), pp. 245-303, Plenum Press, New York

8. Watanabe, Y. (1997) in Oxygenases and model systems (Funabiki, T., ed), pp. 223-282, Kluwer Academic Publishers, Boston

9. Poulos, T. L., Finzel, B. C., and Howard, A. J. (1987) J. Mol. Biol. 195, 687-700

10. Murthy, M. R. N., Reid, T. J., Sicignano, A., Tanaka, N., and Rossmann, M. G. (1981) J. Mol. Biol. 152, 465-499

11. Putnam, C. D., Arvai, A. S., Bourne, Y., and Tainer, J. A. (2000) J. Mol. Biol. 296, 295-309

12. Vainshtein, B. K., Melikadamyan, W. R., Barynin, V. V., Vagin, A. A., Grebenko, A. I., Borisov, V. V., Bartels, K. S., Fita, I., and Rossmann, M. G. (1986) J. Mol. Biol. 188, 49-61

13. Dunford, H. B. (1999) Heme peroxidase, Wiley & Sons, Inc.

14. Everse, J., and Everse, K. E. (1991) Peroxidases in Chemistry and Biology (Grisham, M. B., Ed.), CRC Press, Boca Raton

15. Everse, J., HJohnson, M. C., and Marini, M. A. (1994) Methods in Enzymol. 231, 547-561

16. Sievers, G., and Rünberg, M. C. (1978) B*iochim. Biophys. Acta* **533,** 293-301

17. Matsui, T., Ozaki, S., Liong, E., Phillips, G. N., and Watanabe, Y. (1999) *J. Biol. Chem.* **274,** 2838-2844

PART II

ROLES OF AN ELECTRON-RICH TRYPTOPHAN RESIDUE IN THE HEME ACTIVE SITE

Chapter 1. Effects of an Electron-Rich Tryptophan Residue on The Catalysis.

Chapter 2. Regulation of Substrate Binding in the Heme Enzyme Active Site.

Chapter 1.

Effects of an Electron-Rich Tryptophan Residue on the Catalysis*

*Published in *Biochemistry*, **2000**, *40*, 1044-1502

Molecular Engineering of Myoglobin: The Improvement of Oxidation Activity by Replacing Phe-43 with Tryptophan

Shin-ichi Ozaki, Isao Hara, Toshitaka Matsui, Yoshihito Watanabe

ABSTRACT

The F43W and F43W/H64L Myoglobin (Mb) mutants have been constructed to investigate effects of an electron rich oxidizable amino acid residue in the heme vicinity on oxidation activities of Mb. The Phe-43 $\rightarrow$Trp mutation increases the rate in one-electron oxidation of guaiacol by 3–4-fold; however, the peroxidase activity for F43W/H64L Mb is less than that of the F43W single mutant because the absence of histidine, a general acid-base catalyst, in the distal heme pocket suppresses the compound I formation. More than 15-fold improvement *versus* wild type Mb in the two-electron oxidation of thioanisole and styrene is observed by the Phe-43 $\rightarrow$ Trp mutation. Our results indicate that Trp-43 in the mutants enhances both one- and two-electron oxidation activities (*i.e.* F43W Mb > Wild type Mb and F43W/H64L Mb > H64L Mb). The value of ^{18}O incorporation from $H_2{}^{18}O_2$ into the epoxide product for the wild type is 31 %; however, the values for F43W and F43W/H64L Mb are 75 and 73 %, respectively. Thus, Trp-43 in the mutants does not appear to be utilized as a major protein radical site to form a peroxy protein radical in the oxygenation. The enhanced peroxygenase activity might be explained by the increase in the reactivity of compound I. However, the oxidative modification of F43W/H64L Mb in compound I formation with *m*CPBA prevents us from determining the actual reactivity of the catalytic species for the intact protein. The Lys-C achromobacter digestion of the modified F43W/H64L mutant followed by FPLC and mass analysis identifies that the Trp-43–Lys-47 fragment gains a mass by 30Da, which could correspond two oxygen atoms and loss of two protons.

1.1 INTRODUCTION

Hemoproteins perform a wide variety of functions in biological systems (*1-6*). Among them, myoglobin (Mb), a carrier of molecular oxygen (*7*), is one of the most intensively studied hemoproteins. With the use of multidisciplinary structural and spectroscopic methods, the roles of individual amino acids in regulating ligand affinity (*8-13*) as well as heme binding have been addressed in terms of biological functions (*14-18*).

Myoglobin is also utilized as a framework for molecular engineering studies to probe the structure-function relationships of hemoenzymes (*19*). Careful examination on the location of amino acid residues in the heme vicinity and the peroxide activation mechanism allowed us the rational design of myoglobin mutants transformed into an efficient hemoenzyme by site-directed mutagenesis (*20, 21*). In the catalytic cycle of heme-containing peroxidases, compound I, a ferryl species (Fe^{IV}=O) paired with either porphyrin radical cation or protein radical, is essential for oxidation reactions (*4*). The distal histidine located above the heme iron plays an important role in the formation and reduction of compound I (*4, 22*). Our previous studies indicate that (a) His-64 in wild type Mb destabilizes a ferryl porphyrin radical cation and decreases the catalytic activity (*22*), and (b) the replacement of Phe-43 with a histidine residue, a general-acid base catalyst, accelerates the activation of hydrogen peroxide (Figure 1) (*23*). We constructed the F43H/H64L double mutant to generate compound I efficiently but limit the leakage of an oxidation equivalent from a ferryl porphyrin radical cation through the distal histidine. As we expected, F43H/H64L Mb exhibits up to 300-fold better oxidation activity with respect to the wild type (*23*), and compound I of the mutant shows an absorption spectrum typical for a ferryl porphyrin radical cation (*21*). The X-ray crystal structure of F43H/H64L Mb reveals that the distance between Nε of the distal histidine and the heme iron is 5.7 Å, which is approximately the same as the distance in horseradish peroxidase (HRP) and is longer than that of wild type Mb by 1 Å (*23, 24*). It appears that His-43 in F43H/H64L Mb is not readily oxidized to afford a ferryl species paired with a protein radical (*4, 25*).

On the other hand, a different approach to promote enzymatic activity of myoglobin was also reported (*26*). In wild type Mb, an electron transfer from His-64 to the porphyrin

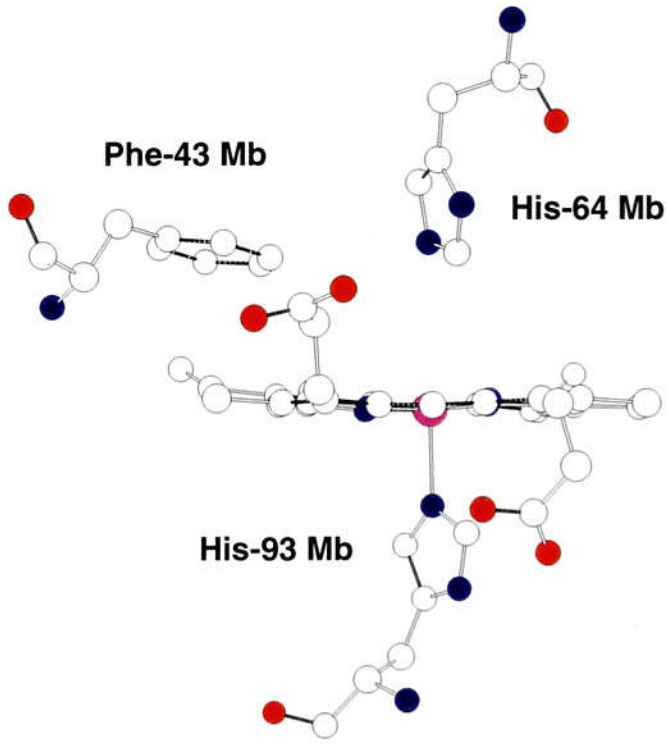

Figure 1. Structure of heme pocket for the ferric wild type sperm whale myoglobin. Heme and some selected amino acid residues including the proximal histidine (His-93) are shown.

radical cation initiates the destabilization of compound I (*21, 22*). The oxidation equivalent temporally stored at the distal histidine is transmitted through several amino acids and relatively stable tyrosine or tryptophan radical is eventually formed (*27*). As a result, one of the oxidation equivalents is completely separated from the heme center, and substrates like styrene are not oxidized efficiently in the heme pocket (*27, 28*). Therefore, Wong *et al.* replaced Phe-43 with a tyrosine residue to retain the second oxidation equivalent as a tyrosine radical in the heme pocket and successfully increased the rate of epoxidation by nearly 30-fold *versus* wild type Mb (*26*). Since a tyrosine is not likely to function as a general acid-base catalyst (pKa = 10), the increase of oxidation activity would be relevant to the enhancement in reactivity of catalytic species.

The improved enzymatic activity observed by the Phe-43 →His (*21*) and Phe-43 →Tyr (*26*) mutation motivated us to introduce a tryptophan, another electron-rich oxidizable residue, at position 43. We have constructed F43W and F43W/H64L Mb and report here that Trp-43

in the mutants increases the one- and two-electron oxidation activity. Furthermore, absorption spectral changes, FPLC, and mass analysis have revealed that the heme pocket of F43W/H64L mutant is oxidatively modified during the reaction with an oxidant, *m*-chloroperbenzoic acid (*m*CPBA).

1.2 EXPERIMENTAL PROCEDURES

Materials. $H_2{}^{18}O_2$ was prepared from $^{18}O_2$ as described by Sawaki and Foote (*29*), and ^{18}O-content of the peroxide was determined to be 92 % by alkaline epoxidation of menadione (*30*). All the other chemicals were purchased from Wako or Nakalai Tesque and used without further purification.

Spectroscopy. All spectroscopic measurements were performed in 50 mM sodium phosphate buffer, pH 7.0, unless indicated. Electronic absorption spectra of purified proteins were recorded on a Shimadzu UV-2400 spectrophotometer. The stopped-flow experiments were performed on a Hi-Tech SF-43 equipped with a MG6000 diode array spectrometer. The Lys-C achromobacter treated proteins were analyzed on ÄKTA FPLC system (Pharmacia), and mass spectra of the fragments were obtained either on a SCIEX (Perkin-Elmer Biosystems, Model API 300) for ESI-MS or Voyager (PerSeptive Biosystems, Model DESTR) for TOF-MS. The both analytical methods provided the same results.

Site-directed Mutagenesis and Protein Purification. The Phe-43 → Trp mutation was introduced by the polymerase chain reaction (PCR) based method. The expression and purification of the mutants were performed as reported previously (*31, 32*). Only a single protein band appeared on a SDS-PAGE gel after the purification procedures.

Measurements of One-electron Oxidation (Peroxidase) Activities. One-electron oxidation activities were measured at 25 °C in 50 mM sodium phosphate buffer, pH 7.0. The typical reaction mixture contained Mb (1 μM) and guaiacol (2 mM). Steady-state kinetic constants were obtained by measuring the initial rates as varying the hydrogen peroxide concentration. The initial rate of guaiacol oxidation was monitored from the increase in absorbance at 470 nm using a molar absorption coefficient of $\varepsilon_{470} = 7.6 \times 10^3$ M^{-}

$^{1}cm^{-1}$ (*23*). At least two sets of experiments were performed to determine the rates.

Measurements of Two-electron Oxidation (Peroxygenase) Activities. The oxidations of thioanisole and styrene were performed at 25 °C in 50 mM sodium phosphate buffer, pH 7.0 (*33*). The reaction mixture contained Mb (10 μM for sulfoxidation and 20 μM for epoxidation), H_2O_2 (1 mM), and either thioanisole (1 mM), or styrene (8.7 mM). For the sulfoxidation assay, acetophenone was added as an internal standard, and the mixture was extracted with dichloromethane for HPLC analysis on a Daicel OD chiral column. The column was eluted with 80 % hexane and 20 % isopropanol at a flow rate of 0.5 mL/min, and the effluent was monitored at 254 nm. For the epoxidation assay, 2-phenyl-2-propanol was added as an internal standard, and the dichloromethane extracts were analyzed by GC (Shimadzu GC-14B) equipped with a Chiraldex G-TA capillary column. The column temperature was kept at 90 °C for the analysis. The standard curves for sulfoxide and epoxide were prepared for quantitative analysis. The rates were determined from the linear portion of the product *versus* time plot, and the absolute stereochemistry was determined on the basis of a retention time of the authentic *S* or *R* product.

Determination of Oxygen Source in the Epoxide Product. The wild type or mutants (20 μM) in 0.5 mL of 50 mM sodium phosphate buffer (pH 7.0) was incubated with styrene (8 mM) and $H_2{}^{18}O_2$ (1 mM) at 25 °C. The dichloromethane extracts of the incubation mixtures were analyzed by GC/MS (Shimadzu GC-17A/GCMS-QP5000) equipped with a Shimadzu CBP1 capillary.

The Formation and Reduction of Compound I of F43W/H64L Mb. The reaction of ferric F43W/H64L Mb with *m*CPBA were performed in 50 mM potassium phosphate buffer (pH 7.4) at 5 °C (*21, 22, 33*). Spectral changes during the compound I formation were recorded on a Hi-Tech SF43 stopped-flow spectrophotometer. The kinetic constants were determined by varying *m*CPBA concentration under the pseudo-first order condition.

The rate of compound I reduction with thioanisole (0.125-1 mM) was measured using a double-mixing rapid scan method in 50 mM potassium phosphate buffer (pH7.4) at 5 °C. In the first mixing, the ferric F43W/H64L Mb reacted with *m*CPBA (20 equivalents with respect to protein) to generate compound I. After the appropriate delay time (0.5 s), thioanisole was

added to compound I to monitor spectral changes. The reaction rate was obtained by fitting the increase in absorbance at 408 nm to a single exponential function.

Characterization of the Modified F43W/H64L Mutant. F43W/H64L Mb (20 μM) was treated with 5 equivalents of *m*CPBA (100 μM) for 10 min at 4 °C in 50 mM potassium phosphate buffer, pH7.4. The mutant treated with *m*CPBA was loaded on a SP-TOYOPEARL 650M column (size: 2.5 ×30 cm), and the modified protein was separated from an excess *m*CPBA and the residual unmodified protein using a linear gradient of 15 mM potassium phosphate (pH 6.0) to 40 mM potassium phosphate (pH 9.0). The typical protein digestion was performed in the presence of myoglobin (600 μg) and Lys-C achromobacter (40 μg) in 100 mM Tris-HCl (pH 9.0) containing 2 M urea, and the mixture was incubated at 25 °C for 12 hours (*34, 35*). The digestion was stopped by adding trifluoroacetic acid (TFA) (final concentration 1%). The digested products were analyzed on a Vydac C-18 reverse phase column eluted at a flow of 0.7 mL/min with a gradient of solvent A (0.1% TFA in water) into solvent B (60 % acetonitrile and 0.07 % TFA in water) over 55 min. The eluent was monitored either at 280 nm for peptides bearing aromatic residues or at 408 nm for heme. Peak fractions were collected and injected directly on a SCIEX (Perkin-Elmer Biosystems, Model API 300) or Voyager (PerSeptive Biosystems, Model DESTR) for mass analysis.

3.3 RESULTS

Absorption Spectra of F43W and F43W/H64L Mb.

The spectra of the ferric, ferrous, and ferrous-CO states of F43W Mb are very similar to the corresponding forms of wild type Mb (Figure 2) (*36*). The Soret band at 408 nm with broad bands at 506 and 635 nm indicates a typical hexa-coordinated ferric high-spin heme (*1*). The sixth ligand in the F43W mutant is a water molecule presumably stabilized by His-64 through hydrogen bonding. Since the loss of water ligation in the ferric F43W/H64L mutant causes a Soret shift to 394 nm (*9*), the novel Trp-43 does not appear to stabilize the heme-bound water. The absorption spectra of the ferrous and ferrous-CO forms of F43W/H64L Mb are essentially identical to those of F43W Mb.

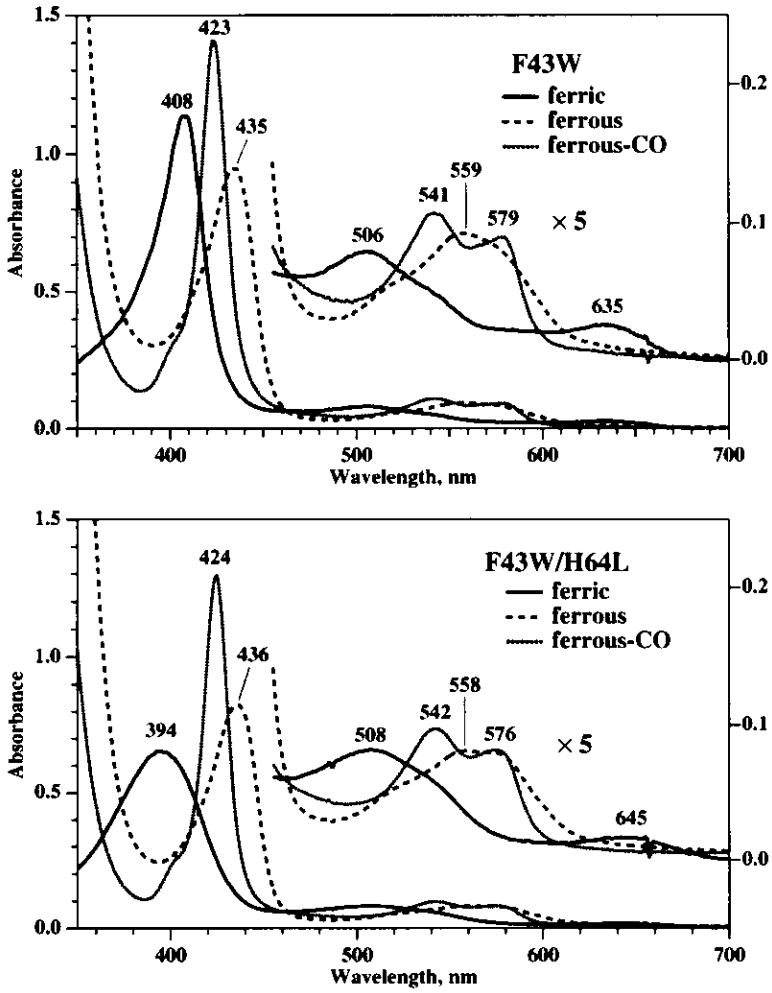

Figure 2. The absorption spectra of the ferric (solid line), ferrous (broken line), and ferrous-CO state (dotted line) for F43W (6 μM) and F43W/H64L Mb (6 μM) in 50 mM sodium phosphate buffer (pH 7.0). The visible region starting at 450 nm is magnified, and the absorbance scale is indicated on the right.

One-electron Oxidation Activities (Peroxidase Activities) of Wild Type Mb and Its Mutants.

One-electron oxidation of guaiacol by the wild type and its mutants was examined in phosphate buffer (pH 7.0) with H_2O_2. With increasing concentrations of H_2O_2, the mutants exhibit a linear increase in the activity; therefore, the rate-determining step for the one-electron oxidation process appears to be the reaction of ferric Mb with H_2O_2. The values in Table 1 are calculated as the slopes of linear portions of the [H_2O_2] *versus* rate plots.

Table 1. Guaiacol Oxidation Catalyzed by Wild Type Mb and its Mutants.

Myoglobin	Guaiacol Oxidation Activity[a]
Wild Type	32
F43W	140
H64L	0.24
F43W/H64L	0.75

[a] All the assays were performed in 50 mM sodium phosphate buffer (pH 7.0). The unit for the oxidation activity is (nmol product)/(nmol Mb)(min)([H_2O_2] mM)

The Phe-43 →Trp mutation increases the one-electron oxidation activity by 3–4-fold: i.e. F43W Mb oxidizes guaiacol approximately 4-fold faster than the wild type, and the F43W/H64L mutant exhibits 3-fold better activity than H64L Mb. Since the proton on the indole nitrogen is not exchangeable, Trp-43 can not function as a general acid-base catalyst like the distal histidine. The deletion of His-64 in F43W Mb decreases the guaiacol oxidation activity by 180-fold. However, the introduction of a tryptophan residue in the active site accelerates the formation of a catalytic species because the rate-determining step for one-electron oxidation reaction is found to be compound I formation. The indole proton in the active site might increase the affinity with H_2O_2 through hydrogen bond.

Two-electron Oxidation Activities (Peroxygenase Activities) of Wild Type Mb and Its Mutants.

Two-electron oxidations, a ferryl oxygen transfer to thioanisole and styrene, have also been examined (Table 2). F43W Mb exhibits the best two-electron oxidation activity as observed for guaiacol oxidation. The Phe-43 Trp mutation results in the enhancement in oxygenation activities (*i.e.* F43W Mb > Wild type Mb and F43W/H64L Mb > H64L Mb), and His-64 in myoglobins improves the two-electron oxidation reactions (i.e. F43W Mb > F43W/H64L Mb and Wild type Mb > H64L Mb). The trends here are essentially the same

as for one-electron oxidation, but the degree in activity enhancement by the tryptophan mutation is different. Approximately 20-fold improvement in the rate of sulfoxidation and epoxidation is observed by the replacement of Phe-43 in wild type Mb with a tryptophan residue. The F43W/H64L mutant oxidizes thioanisole 26-fold faster than H64L Mb. The 15–26-fold increase in two-electron oxidation activity is greater than the enhancement observed for one-electron oxidation of guaiacol (c.a. 3—4-fold). The results suggest that the reaction of ferric Mb with H_2O_2 is not the only step controlling the rate of oxygenation reaction. The reactivity of compound I with thioanisole and styrene might be increased by the replacement of Phe-43 with a tryptophan residue.

Table 2. Enantioselective Oxidation of Thioanisole and Styrene by wild type, F43W, H64L, and F43W/H64L Mb[a].

	Thioanisole		Styrene	
	rate (min^{-1})	% ee	rate (min^{-1})	% ee
Wild Type	0.64	24	0.011	15
F43W	13	30	0.16	48
F43W/H64L	1.9	24	0.11	50
H64L	0.072	27	0.020	34

[a]The absolute stereochemistry of the dominant isomer for sulfoxide and epoxide is *R*.

The Phe-43 Trp mutation does not appear to create a specific binding site to produce one of the isomers with high enantioselectively (Table 2). F43H/H64L Mb (85 % ee and 68 % ee for sulfoxidation and epoxidation, respectively) is found to be a better chiral catalyst than the F43W/H64L mutant. Although clear rationalization for stereoselectivity in the oxidation system with Mbs has not been provided at the moment, the amino acid at position 43 appears to be one of the important residues for asymmetric oxidations.

In order to estimate the ratio of a ferryl oxygen transfer *versus* a peroxy protein radical mechanism, ^{18}O-labeled H_2O_2 was used to perform the reaction (Table 3). More than 87 %

^{18}O incorporation into the methyl phenyl sulfoxide suggests that a ferryl oxygen transfer mechanism is favored in the sulfoxidation reaction. The low ^{18}O incorporation into the epoxide product for the wild type was explained by a peroxy protein radical mechanism, and Trp-14 eventually bearing one of the oxidation equivalents was recently suggested to be a stable radical site (*27*). As a result, the oxygen atom of epoxide is derived from molecular oxygen. The ^{18}O incorporation increases from 31 to 73 % by the His-64 Leu mutation presumably because an unoxidizable Leu-64 partially prevents leakage of one of the oxidation equivalents from compound I to form the protein radical. Since the value for F43W/H64L Mb is the same as that of the H64L mutant, Trp-43 does not seem to promote a peroxy protein radical mechanism. In the F43W mutant, the two different oxidation mechanisms could compete; however, 75 % incorporation is essentially the same as the values for F43W/H64L and H64L Mb. Thus, compound I of F43W Mb seems to oxidize styrene before losing its oxidation equivalents through His-64. The result might imply the increase in reactivity of compound I by the Phe-43 $\rightarrow$Trp mutation in the active site.

Table 3. Origins of the Oxygen Atom in the Sulfoxide and Epoxide Product.

	% ^{18}O incorporation from $H_2{}^{18}O_2$			
	Wild Type	F43W	F43W/H64L	H64L
Sulfoxidation	87	92	91	89
Epoxidation	31	75	73	73

Styrene is oxidized not only to styrene oxide but also to benzaldehyde and phenylacetaldehyde (Table 4). Benzaldehyde is produced in the H_2O_2-supported oxidation of styrene by most hemoproteins via unknown mechanism, but phenylacetaldehyde is formed by a hydrogen rearrangement reaction (*37-39*). Since the proton transfer to the benzylic carbon would be favored in a polar active site, the ratios of these three products could help us estimate the polarity of heme pocket. Phenylacetaldehyde accounts for only 6 % of the total products for H64L Mb, and the ferric state of the mutant is known to be in the penta-

coordinated state, where a water molecule is not bound to the iron (*9*). The percentages of phenylacetaldehyde are 25 % (wild type Mb), 61 % (F43W Mb), and 52 % (F43W/H64L Mb), which are greater than the values for H64L Mb. Although the absorption spectrum of F43W/H64L Mb indicates that a water molecule is not coordinated to the heme iron, there might be some water molecules stabilized by Trp-43 (*i.e.* N-H of the indole moiety) through hydrogen bond in the heme pocket.

Table 4. Products Formed in the Reaction of Styrene with wild type, F43W, and F43W/H64L Mb[a].

	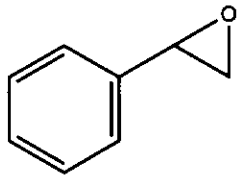 styrene oxide	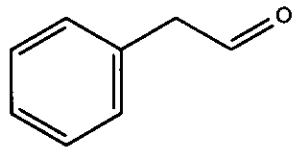 phenylacetaldehyde	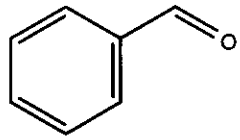 benzaldehyde
Wild Type	57 %	25 %	18 %
F43W	34	61	5
F43W/H64L	42	52	6

[a]The oxidized product ratios are reported in percent.

The Formation and Reduction of Compound I.

The results of two-electron oxidation activities suggest that the Phe-43 Trp mutation might increase the reactivity of compound I. In order to examine the implication, we decided to determine the rate of compound I reduction for F43W/H64L Mb in the presence of thioanisole using a stopped-flow apparatus. Compound I can be observed in the His-64 deletion mutants when *m*CPBA is used as an oxidant because the distal histidine lies in a path for the oxidation equivalents to leak out (*22*). The absence of a general-acid catalyst in the mutants can be compensated by the use of *m*CPBA bearing carboxylate moiety as a good leaving group to achieve the heterolytic cleavage of the oxygen-oxygen bond.

Typical absorption spectral changes upon the mixing of the F43W/H64L mutant and

*m*CPBA are shown in Figure 3 (A). Addition from 10 to 50 equivalents of *m*CPBA to F43W/H64L Mb with a Soret maximum at 394 nm, first produces a sharp and more intense Soret band at 408 nm. Then, the spectrum changes to a typical compound I spectrum with approximately 2-fold decrease in the Soret intensity with intense absorbance around 500-700 nm. The kinetic constant (k_1) for the formation of an intermediate (compound X) with λ_{max} = 408 nm is 1.3×10^5 $M^{-1}s^{-1}$ (Figure 3 (B)). The rate of compound I formation is also proportional to the concentration of *m*CPBA, and the kinetic constant (k_2) is 1.9×10^4 $M^{-1}s^{-1}$ (Figure 3 (B)).

The reduction of F43W/H64L Mb compound I with thioanisole causes an increase in absorbance at 408 nm with no shift of the Soret band ($k_3 = 4.5 \times 10^5$ $M^{-1}s^{-1}$) (Figure 4). The spectrum after the reduction is essentially the same as that of compound X, and compound I of F43W/H64L Mb has never been reduced to a penta-coordinated ferric form with the Soret band at 394 nm. In compound I formation with *m*CPBA, *m*-chlorobenzoic acid (*m*CBA), which could be bound to the ferric heme iron, is produced as a side product. However, mixing the F43W/H64L mutant with *m*CBA does not shift a Soret band from 394 nm to 408 nm. Therefore, the species with λ_{max} = 408 nm (compound X) seems to be the hexa-coordinated ferric high spin state heme with a water molecule as the sixth ligand.

Characterization of Compound X.

Compound X is generated simultaneously by adding approximately two equivalents of *m*CPBA to F43W/H64L Mb, and the species is stable enough to be observed and isolated at the room temperature. In order to ascertain features of compound X, several experiments were performed.

We first generated compound X and then added potassium cyanide. If compound X is a heme-*m*CPBA adduct, a ligand exchange occurs to form a cyanide-heme iron complex. It would be possible to titrate the amount of *m*CPBA with potassium iodide (Scheme 1). Upon the addition of potassium cyanide, we observed a red-shift of the Soret band, which is an indication of cyanide complex formation. However, iodide was not oxidized to triiodide because there was no increase in absorbance at 353 nm for I_3^-.

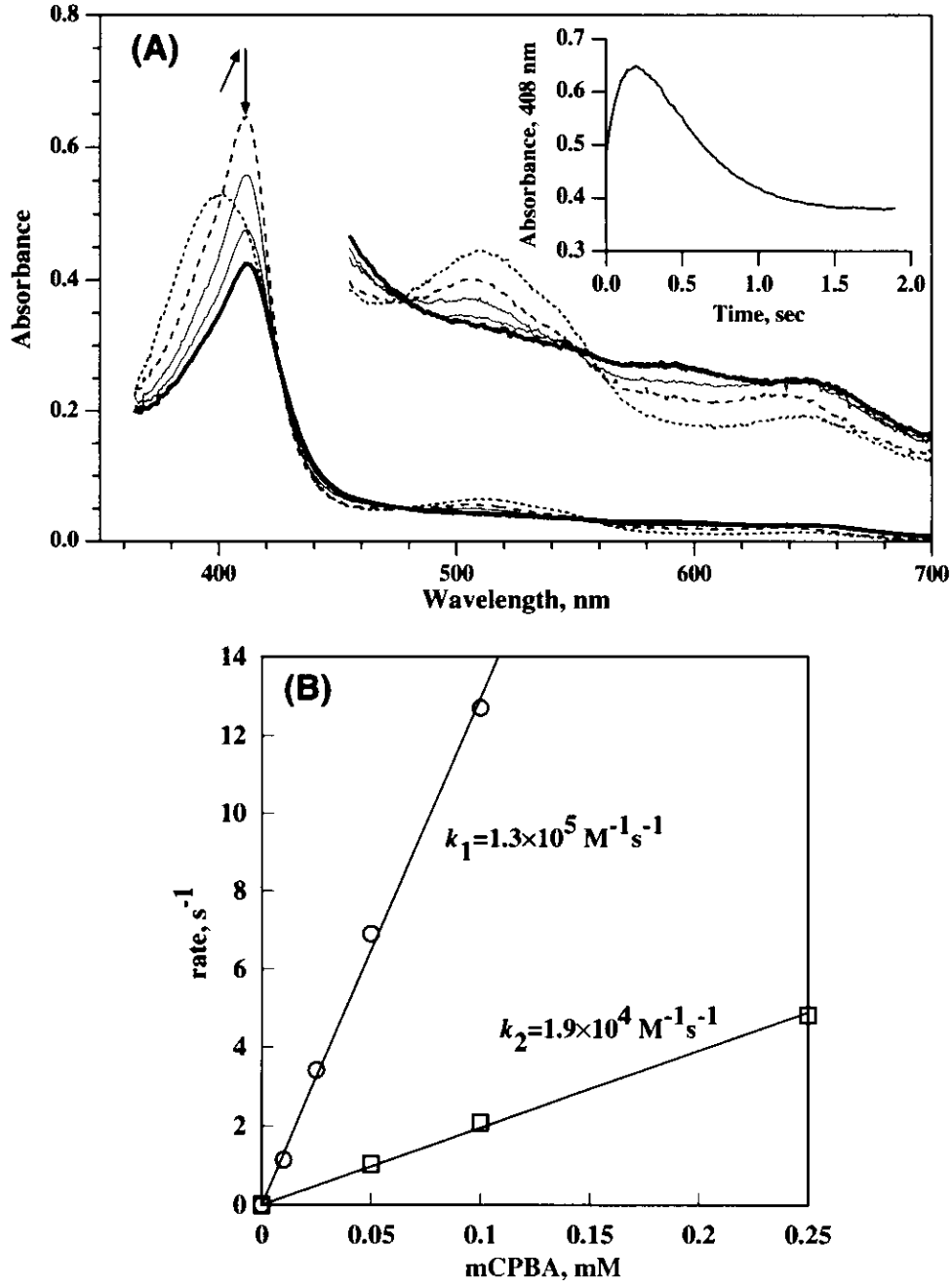

Figure 3. (A) Absorption spectral changes of F43W/H64L Mb upon mixing with *m*CPBA. The dotted line and thick line represent the initial ferric state and compound I, respectively. The dashed line is an intermediate, compound X, observed prior to the compound I formation. Inset: The absorbance changes at 408 nm *versus* time. The visible region starting at 450 nm is magnified, and the absorbance scale is indicated on the right. (B) The plots of [*m*CPBA] *versus* the rate of compound X formation or compound I formation. The rate constants (k_1 and k_2) were determined as the slopes.

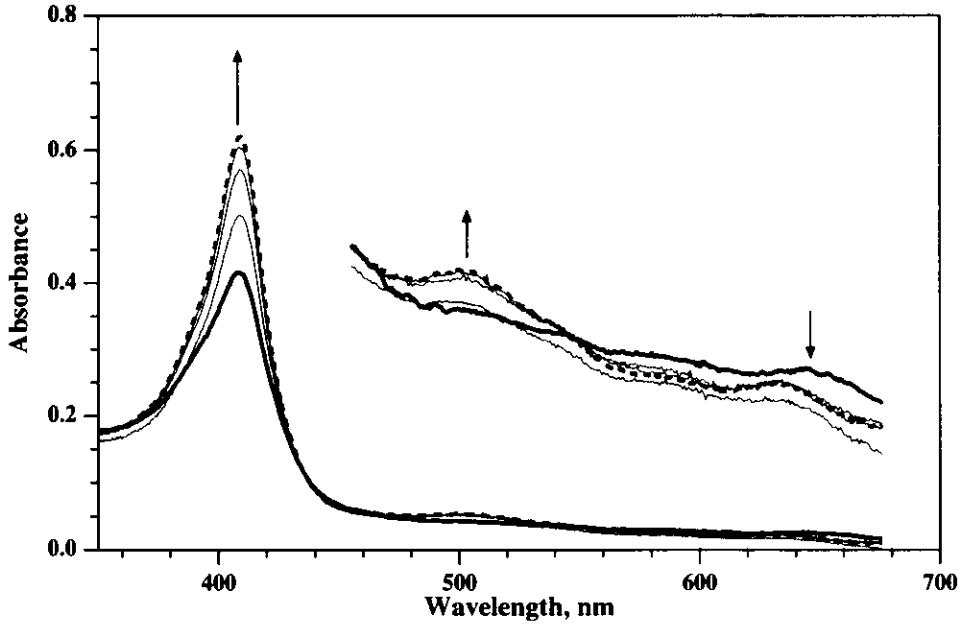

Figure 4. Reduction of compound I for F43W/H64L Mb in the presence of thioanisole. Arrows indicate directions of absorbance changes. The thick line indicates compound I immediately after the mixing, and the dashed line represents the ferric state (8 msec after adding thioanisole). The spectra taken every 2 msec are shown. The visible region starting at 450 nm is magnified, and the absorbance scale is indicated on the right.

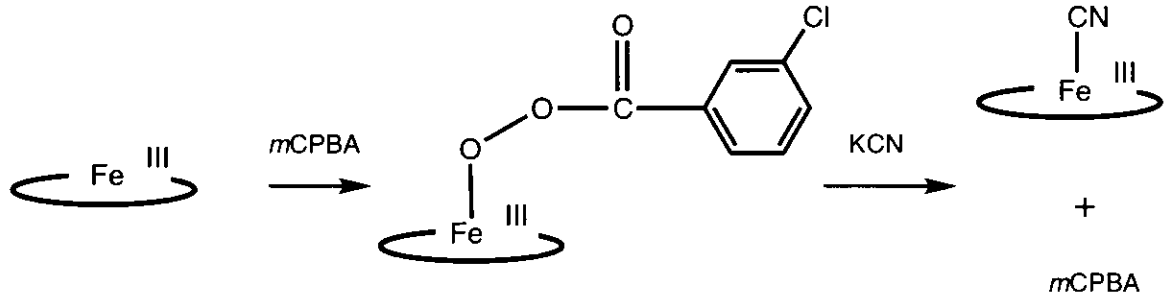

Scheme 1

Since tri-iodide would react with amino acid like a tyrosine residue in the protein, we further attempted to quantitate *m*CPBA, if it is released from compound X, with thioanisole. Thioanisole is simultaneously oxidized in the presence of stoichiometric amount of *m*CPBA, and the sulfoxide product is analyzed by HPLC. In the experiment, an excess of potassium cyanide (20 mM) was added to compound X (20 μM) and the cyanide complex formation was confirmed by the absorption spectrum. Then, thioanisole (1 mM) was added to the solution; however, the sulfoxide product was not observed in the dichloromethane extract.

The results suggest that (a) a ligand originally bound to the heme iron in compound X can exchange with cyanide, (b) *m*CPBA is not released from compound X upon the addition of potassium cyanide, (c) compound X does not have oxidizing equivalents. Although direct evidence like the crystal structure is necessary to conclude structural features of compound X, our observations imply that compound X does not seem to be a highly reactive heme-*m*CPBA complex. We speculated that chemical modifications of the F43W/H64L mutant by *m*CPBA cause structural changes in the heme pocket. If the oxygenation of the active site residues occurs, a water molecule bound to the heme iron as the sixth ligand could be stabilized through hydrogen bonding interaction. We hypothesize that compound X is in the ferric high spin state with a water molecule as the distal ligand.

In order to examine our hypothesis and identify the modification site, we treated F43W/H64L Mb with Lys-C achromobacter, separated the digested products by FPLC, and then determined the molecular weights of the peptide fragments by ESI-MS and TOF-MS. The F43W/H64L mutant yielded four major fragment peaks in the FPLC chart when monitored at 280 nm, which are assigned to peptides (1) Tyr-146–Lys-147, (2) Glu-148–Gly-153, (3) Trp-43–Lys-47, (4) a mixture of Val-1–Lys-16 and Tyr-103–Lys-133 in the elution order by mass analysis (Figure 5A). All the fragments bearing aromatic residues were identified in the control experiment. In addition, the heme released from the protein is found to be eluted at 62 min by monitoring at 408 nm (Figure 5C,D).

In the chromatograph of *m*CPBA treated F43W/H64L Mb, two new peaks indicated by asterisk appear before the Trp-43–Lys-47 peptide (WDRFK) elutes, and the peak assigned to the intact WDRFK fragment is diminished (Figure 5B). Both of the new adducts have a mass of 781.4 Da, which is greater than the molecular weight of Trp-43–Lys-47 fragment by 30 Da (Figure 6). Furthermore, the MS-MS analysis of the mCPBA treated Trp-43–Lys-47 fragment suggests that Trp-43 is the exact modification site. The results suggest that 1) the reaction of F43W/H64L Mb with *m*CPBA produces two different adducts, 2) the modification site is Trp-43, and 3) the increase in mass by 30 Da after the reaction could be associated with the addition of two oxygen atoms and the loss of two protons. The addition of polar oxygen atoms is consistent with the shorter retention times of the modified adducts than that of the

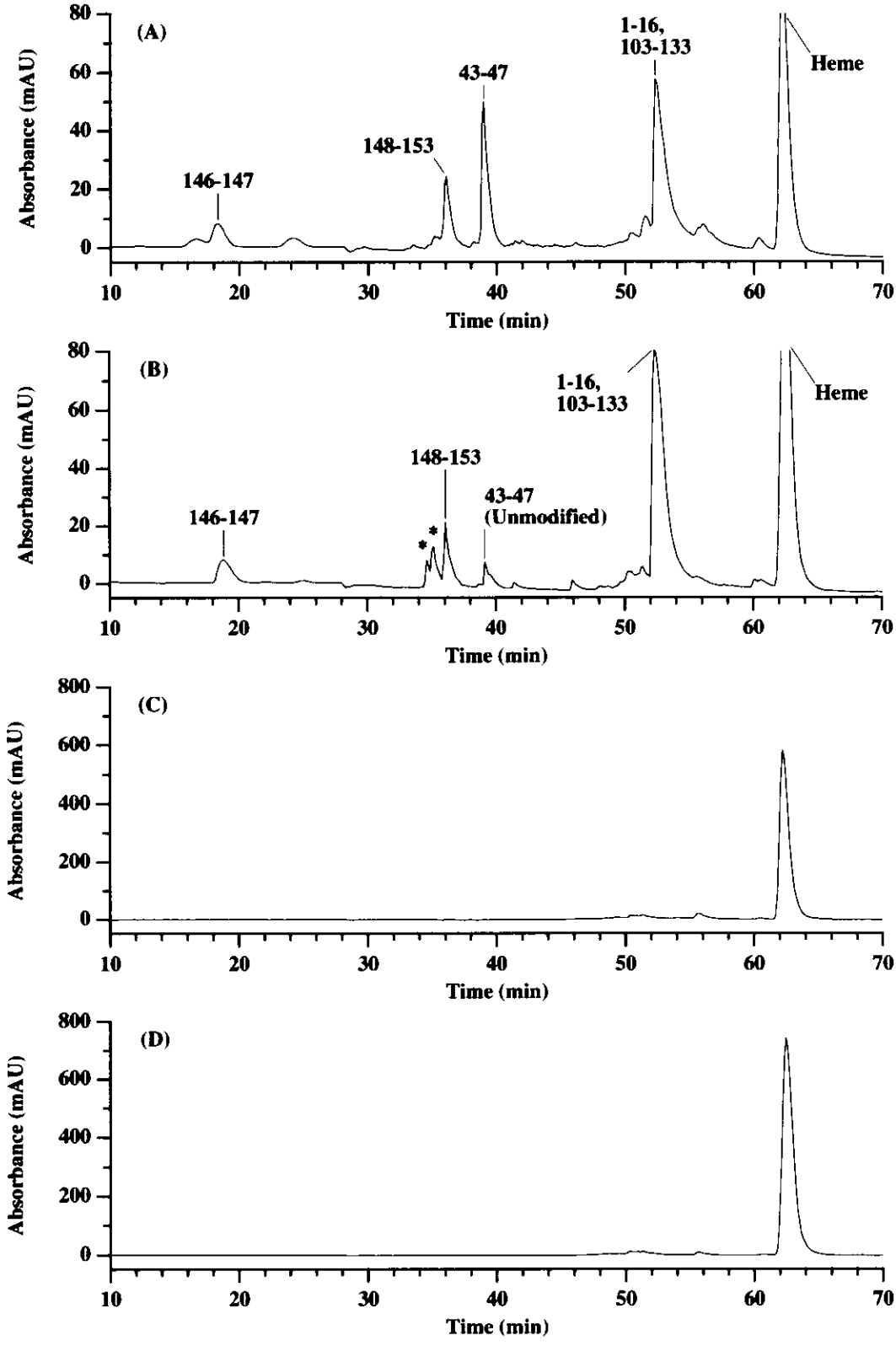

Figure 5. FPLC-profile of Lys-C achromobacter treated F43W/H64L Mb ((A) and (C)) and Lys-C achromobacter treated F43W/H64L Mb after reaction with *m*CPBA ((B) and (D)). The traces monitored at 280 nm ((A) and (B)) and 408 nm ((C) and (D)) were shown.

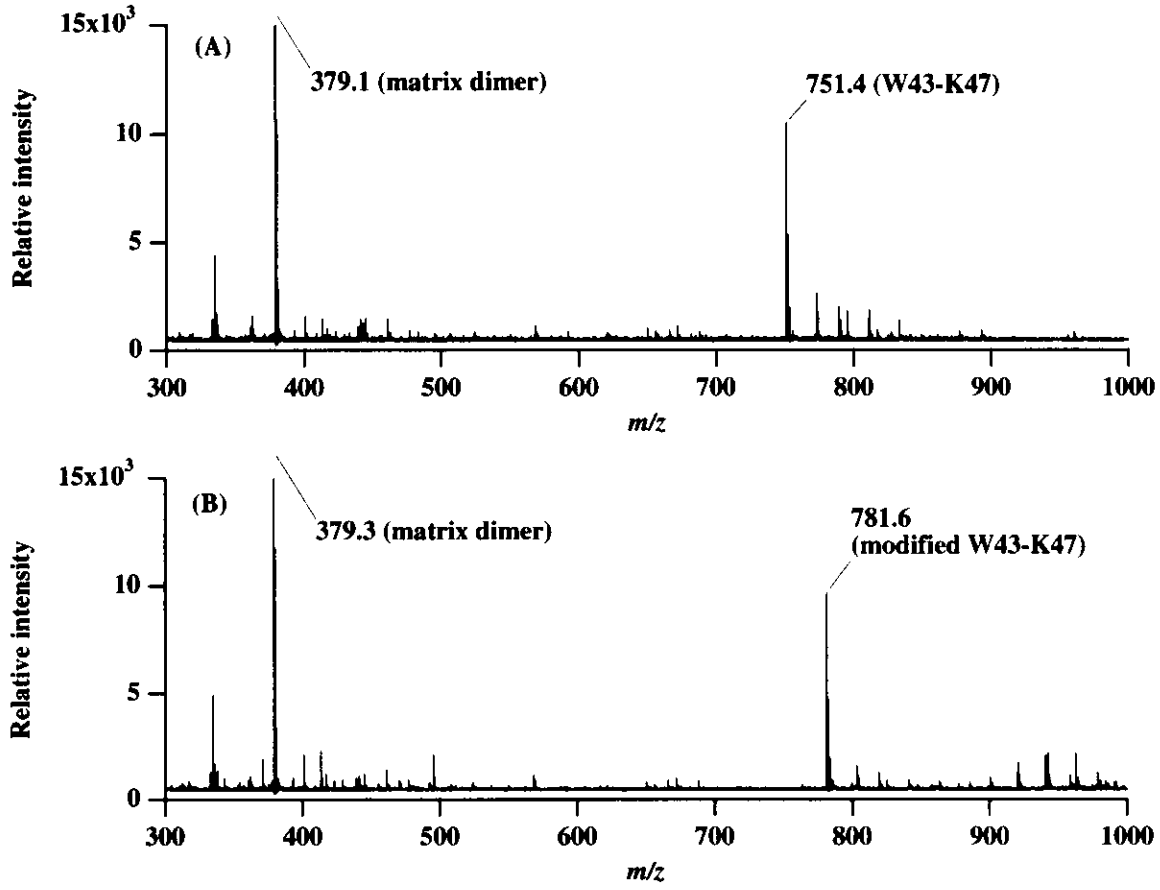

Figure 6. TOF-MS spectrum of (A) Trp-43–Lys-47 and (B) Trp-43–Lys-47 treated with *m*CPBA.

intact Trp-43–Lys-47 fragment. Furthermore, the absorption spectral changes from penta- to hexa-coordinated high spin state upon the reaction with *m*CPBA could also be rationalized by the stabilization of a water molecule bound to the heme iron through hydrogen bonding interaction with the oxygenated amino acid residues. Although the autocatalytic hydroxylation at β carbon of Trp-171 in lignin peroxidase has recently been reported (*40, 41*), the similar mechanism may not be applied in the myoglobin mutant. We speculate at the moment that the tryptophylquinone isomers are produced because the absorption spectrum of the modified Trp-43–Lys-47 fragment (λmax at 397 nm) is similar to those of indole quinone model compounds previously synthesized (*42*). Further studies on the exact structure of heme pocket for the modified F43W/H64L mutant as well as the oxygenation mechanism are now under way.

3.4 DISCUSSION

The results presented here indicate that the replacement of Phe-43 with Trp enhances both one- and two-electron oxidation activities. In the one-electron process, compound I formation is the rate-determining step, and Trp-43 in the active site of the mutants accelerates the reaction of ferric Mb with H_2O_2 (Table 1). The hydrogen-bonding interactions through the indole ring as well as the polar heme environment might favor the activation of H_2O_2 to generate compound I efficiently (*43*). The tryptophan side chain, however, can not function as a general acid-base catalyst. Therefore, the absence of the distal histidine in the F43W/H64L mutant suppresses the one-electron oxidation of guaiacol with respect to the wild type.

On the other hand, compound I formation does not seem to be the sole rate-determining step in the two-electron process. The Phe-43 Trp single replacement facilitates the epoxidation and sulfoxidation by 15–25-fold, which is in the similar degree as observed for the Phe-43 His and Phe-43 Tyr mutation (*21, 26*), but the mutation increases the rate of compound I formation only by 3–4-fold (Table 2). Furthermore, the ferryl oxygen transfer process is slower than one-electron oxidation reaction. The enhanced activity for the tryptophan mutants would not be due to the increase in substrate accessibility because a tryptophan residue is larger than a phenylalanine. In order to examine if the reactivity of compound I is improved by the Phe-43 Trp mutation, we performed a single turnover experiment on a stopped flow apparatus. In the experiment, compound I of F43W/H64L Mb was first generated using *m*CPBA as an oxidant, and then thioanisole was mixed to measure the reduction rate. The rate constant for compound I reduction with thioanisole (k_3) is 4.3 $\times 10^5$ $M^{-1}s^{-1}$. The value is slightly greater than that for H64L Mb (k_3 = 3.1 $\times 10^5$ $M^{-1}s^{-1}$) but does not seem to be large enough to account for the 26-fold enhancement in sulfoxidation activity by the Phe-43 Trp / His-64 Leu double mutation.

However, the absorption spectral changes during the reaction of F43W/H64L Mb with *m*CPBA suggest that the penta-coordinated ferric high spin state is transformed into the hexa-coordinated ferric high spin state (compound X) prior to the compound I formation (Figure 3). Characterization of compound X by FPLC and mass analysis reveals that the active site of the

F43W/H64L mutant is oxidatively modified. Thus, the rate of compound I reduction determined here is not for the intact but for the modified F43W/H64L mutant.

Although the exact structure of the modified Trp-43–Lys-47 fragment remains to be elucidated, there is no doubt that the substitution of Phe-43 with a tryptophan residue causes the modification of the active site in the presence of *m*CPBA as an oxidant. The tryptophylquinone-like structure we propose here is still no more than speculation, but tryptophan tryptophylquinone (TTQ) is known as a covalently bound cofactor for methylamine dehydrogenase (MADH) (*44-46*).

In summary, the replacement of Phe-43 with a tryptophan residue enhances one- and two-electron oxidation activities (i.e. F43W Mb > Wild type Mb and F43W/H64L Mb > H64L Mb). Our results support the hypothesis that an electron-rich oxidizable residue at position 43 would improve the catalytic activity. The improved peroxidase activity (i.e. one-electron process) is due to the acceleration in compound I formation. The enhanced peroxygenase activity (i.e. two-electron process) might be explained by the increase in the reactivity of compound I. However, the rationalization remains to be proved because the oxidative modification of F43W/H64L Mb in compound I formation with *m*CPBA prevents us from determining the actual reactivity of the catalytic species for the intact protein. Finally, the combinations of FPLC and MS analysis allow us to identify that Trp-43 gains a mass by 30 Da due to the post-translational modification. The further mechanistic studies on the myoglobin's post-translational modification such as the source of oxygen atoms of the modified adducts are awaited.

3.5 REFERENCES

1. Antonini, E., and Brunori, M. (1971) *Hemoglobin and Myoglobin in Their Reactions with Ligands*, North-Holland Publishing Co., Amsterdam.
2. Ho, C. (1982) *Hemoglobin and Oxygen Binding*, Elsevier, New York.
3. Moore, G. R., and Pettigrew, G. W. (1990) *Cytochromes C*, Springer-Verlag, New York.

4. Everse, J., Everse, K. E., and Grisham, M. B. (1991) *Peroxidases in Chemistry and Biology*, Vol. I & II, CRC Press, Boca Raton.

5. Lippard, S. J., and Berg, J. M. (1994) *Principles of Bioinorganic Chemistry*, University Sciences Books, Mill Valley, California.

6. Ortiz de Montellano, P. R. (1995) *Cytochrome P450*, Vol. 2nd Ed., Plenum Press:, New York.

7. Wittenberg, B. A., Wittenberg, J. B., and Caldwell, P. R. B. (1975) *J. Biol. Chem. 250*, 9038-9043.

8. Carver, T. E., Rohlf, R. J., Olson, J. S., Gibson, Q. H., Blackmore, R. S., Springer, B. A., and Sligar, S. G. (1990) *J. Biol. Chem. 265*, 3168-3176.

9. Quillin, M. L., Arduiini, R. M., Olson, J. S., and Phillips, G. N. (1993) *J. Mol. Biol. 234*, 140-155.

10. Ikeda-Saito, M., Dou, Y., Yonetani, T., Olson, J. S., Li, T., Regan, R., and Gibson, Q. H. (1993) *J. Biol. Chem. 268*, 6855-6857.

11. Sakan, Y., Ogura, T., Kitagawa, T., Fraunfelder, F. A., Mattera, R., and Ikeda-Saito, M. (1993) *Biochemistry 32*, 5815-5824.

12. Cameron, A. D., Smerdon, S. J., Wilkinson, A. J., Habash, J., Helliwell, J. R., Li, T., and Olson, J. S. (1993) *Biochemistry 32*, 13061-13070.

13. Krzywda, S., Murshudov, G. N., Brzozowski, A. M., Jaskolski, M., Scott, E. E., Klizas, S. A., Gibson, Q. H., Olson, J. S., and Wilkinson, A. J. (1998) *Biochemistry 37*, 15896-15907.

14. Hughson, F. M., and Baldwin, R. L. (1989) *Biochemistry 28*, 4415-4422.

15. Hargrove, M. S., Singleton, E. W., Quillin, M. L., Ortiz, L. A., Phillips, G. N., Mathews, A. J., and Olson, J. S. (1994) *J. Biol. Chem. 269*, 4207-4214.

16. Hargrove, M. S., Krzywda, S., Wilkinson, A. J., Dou, Y., Ikeda-Saito, M., and Olson, J. S. (1994) *Biochemistry 33*, 11767-11775.

17. Hargrove, M. S., and Olson, J. S. (1996) *Biochemistry 35*, 11310-11318.

18. Kiefhaber, T., and Baldwin, R. L. (1996) *J. Mol. Biol. 252*, 122-132.

19. Ozaki, S., Matsui, T., Roach, P. M., and Watanabe, Y. (2000) *Coord. Chem. Rev. 198*, 39-59.

20. Ozaki, S., Matsui, T., and Watanabe, Y. (1996) *J. Am. Chem. Soc. 118*, 9784-9785.

21. Ozaki, S., Matsui, T., and Watanabe, Y. (1997) *J. Am. Chem. Soc. 119*, 6666-6667.

22. Matsui, T., Ozaki, S., and Watanabe, Y. (1997) *J. Biol. Chem. 272*, 32735-32738.

23. Matsui, T., Ozaki, S., Liong, E., Phillips, G. N., and Watanabe, Y. (1999) *J. Biol. Chem. 274*, 2838-2844.

24. Phillips, G. N. J., Arduini, R. M., Springer, B. A., and Sligar, S. G. (1990) *Proteins: Struct. Funct. Genet. 7*, 358-365.

25. Huyett, J. E., Doan, P. E., Gurbiel, R., Houseman, A. L. P., Sivaraja, M., Goodin, D. B., and Hoffman, B. M. (1995) *J. Am. Chem. Soc. 117*, 9033-9041.

26. Levinger, D. C., Stevenson, J.-A., and Wong, L.-L. (1995) *J. Chem. Soc. Chem. Commun.*, 2305-2306.

27. DeGray, J. A., Gunther, M. R., TschirretGuth, R., Oritiz de Montellano, P. R., and Mason, R. P. (1997) *J. Biol. Chem. 272*, 2359-2362.

28. Catalano, C. E., Choe, Y. S., and Ortiz de Montellano, P. R. (1989) *J. Biol. Chem. 264*, 10534-19541.

29. Sawaki, Y., and Foote, S. T. (1979) *J. Am. Chem. Soc. 101*, 6292-6296.

30. Ortiz de Montellano, P. R., and Catalano, C. E. (1985) *J. Biol. Chem. 260*, 9265-9271.

31. Springer, B. A., and Sligar, S. G. (1987) *Proc. Natl. Acad. Sci. U.S.A. 84*, 8961-8965.

32. Springer, B. A., Egeberg, K. D., Sligar, S. G., Rohlfs, R. J., Mathews, A. J., and Olson, J. S. (1989) *J. Biol. Chem. 264*, 3057-3060.

33. Ozaki, S., Yang, H.-J., Matsui, T., Goto, Y., and Watanabe, Y. (1999) *Tetrahedron: Asymmetry*, 183-192.

34. Fenwick, C. W., and English, A. M. (1996) *J. Am. Chem. Soc. 118*, 12236-12237.

35. Tschirret-Guth, R. A., Medzihradszky, K. F., and Ortiz de Montellano, P. R. (1998) *J. Am. Chem. Soc. 120*, 7404-7410.

36. Takano, T. (1977) *J. Mol. Biol. 110*, 537-568.

37. Miller, V. P., DePillis, G. D., Ferrer, J. C., Mauk, A. G., and Ortiz de Montellano, P. R. (1992) *J. Biol. Chem. 267*, 8939-8942.

38. Rao, S. I., Wilks, A., and Ortiz de Montellano, P. R. (1993) *J. Biol. Chem. 268*, 803-

809.

39. Ozaki, S., and Ortiz de Montellano, P. R. (1995) *J. Am. Chem. Soc. 117*, 7056-7064.

40. Blodig, W., Doyle, W. A., Smith, A. T., Winterhalter, K., Choinowowski, T., and Piontek, K. (1998) *Biochemistry 37*, 8831-8838.

41. Blodig, W., Smith, A. T., Winterhalter, K., and Piontek, K. (1999) *Arch. Biochem. Biophys. 370*, 86-92.

42. Moënne-Loccoz, P., Nakamura, N., Itoh, S., Fukuzumi, S., Gorren, A. C. F., Duine, J. A., and Sanders-Loehr, J. (1996) *Biochemistry 35*, 4713-4720.

43. Matsui, T., Ozaki, S., and Watanabe, Y. (1999) *J. Am. Chem. Soc. 121*, 9952-9957.

44. Chen, L., Mathews, F. S., Davidson, V. L., Huizinga, E. G., Vellieux, F. S., Duine, J. A., and Hol, W. G. J. (1991) *FEBS Letters 287*, 163-166.

45. McIntire, W. S., Wemmer, D. E., Chistoserdov, A. E., and Lidstrom, M. E. (1991) *Science 252*, 817-824.

46. Tanizawa, K. (1995) *J Biochem 118*, 671-678.

Chapter 2.

Regulation of Substrate Binding in the Heme Active Site*

*J. Biol. Chem, **2001**, 271, 36067-36070

Oxidative Modification of Tryptophan-43 in the Heme Vicinity of the F43W/H64L Myoglobin Mutant

Isao Hara, Takafumi Ueno, Shin-ichi Ozaki, Shinobu Itoh, Keonil Lee, Norikazu Ueyama, and Yoshihito Watanabe

ABSTRACT

The F43W/H64L myoglobin mutant was previously constructed to investigate the effects of electron-rich tryptophan residue in the heme vicinity on the catalysis, where we found that Trp-43 in the mutant was oxidatively modified in the reaction with *m*-chloroperbenzoic acid (*m*CPBA). To identify the exact structure of the modified tryptophan in this study, the *m*CPBA-treated F43W/H64L mutant has been digested stepwise with Lys-C achromobacter and trypsin to isolate two oxidation products by preparative FPLC. The close examinations of the ^{1}H NMR spectra of peptide fragments reveal that two forms of the modified tryptophan must have 2,6-disubstituted indole substructures. The ^{13}C NMR analysis suggests that one of the modified tryptophan bears a unique hydroxyl group in stead of the NH_2 group at the amino-terminal. The results together with mass spectrometry (MS)/MS analysis (30 Da increase in mass of Trp-43) indicate that oxidation products of Trp-43 are 2,6-dihydro-2,6-dioxoindole and 2,6-dihydro-2-imino-6-oxoindole derivatives. Our finding is the first example of the oxidation of aromatic carbons by the myoglobin mutant system.

2. 1 INTRODUCTION

Myoglobin (Mb), a carrier of molecular oxygen, can perform oxidation reactions in the presence of hydrogen peroxide (H_2O_2) although the activity is not as great as that of peroxidase.(1-3) The accumulated biochemical and biophysical data allow us to utilize Mb as a heme enzyme model system, and various myoglobin mutants have been constructed to elucidate structure–function relationship on the activation of peroxides.(3-5) For example, F43H/H64L Mb, one of the distal histidine relocation mutants, exhibits the enhanced reactivity with H_2O_2 and the longer lifetime of an active intermediate, a ferryl porphyrin radical cation ($O=Fe^{IV}$porphyrin$^{\bullet+}$).(6) Therefore, the F43H/H64L mutant is able to catalyze the sulfoxidation and epoxidation reaction at the rate comparable to the values of peroxidases.

On the other hand, cytochromes P-450 (P-450) catalyze the hydroxylation of a wide variety of substrates including hydrocarbons and polycyclic aromatic molecules.(7,8) The variance in reactivity of Mb and P-450 could arise from differences in the active site structure and the arrangement of functional amino acid residues. The crystal structure of P-450cam with *d*-camphor reveals that the substrate is tightly bound in the hydrophobic heme pocket through hydrogen bonding interaction with the hydroxyl group of Tyr-96 and the carbonyl oxygen of *d*-camphor **(Figure 1A)**.(9) The distance between the heme iron and C5 of *d*-camphor, the hydroxylation site, is 4.2 Å. On the contrary, the active site of myoglobin is exposed to the exterior and does not provide any specific interactions for accommodating a foreign substrate with high affinity.(10) Therefore, it will be difficult for a ferryl porphyrin radical cation of Mb to hydroxylate a substrate molecule, which is not bound in an appropriate position nearby the heme. We hypothesize that a ferryl oxygen atom transfer to aliphatic or aromatic molecules by Mb mutants might be possible even without a proximal thiolate ligand if the substrates were fixed nearby the heme iron.

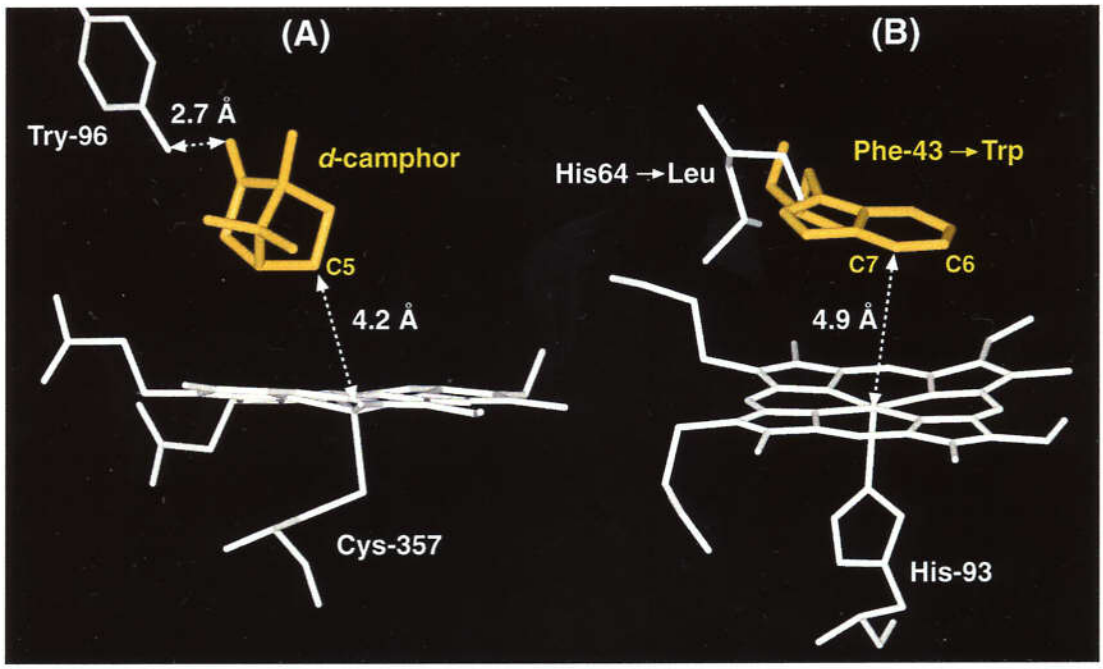

Figure 1. (A) Crystal structure of P450cam and (B) calculated structure of F43W/H64L Mb. Trp-43 and the substrate camphor are shown in yellow.

The F43W/H64L Mb mutant, which was previously constructed to investigate effects of an electron-rich tryptophan residue on the peroxygenase activity, appears to be a good model for examining the hypothesis because aromatic carbon atoms of tryptophan are fixed in the heme vicinity (**Figure 1B**).(11) Although the crystal structure of the F43W/H64L Mb mutant is not available at the moment, the calculated model structure suggests that the distances of Fe–C7 and Fe–C6 are 4.9 and 5.5 Å, respectively. (A calculated structure of F43W/H64L Mb was obtained by using the Insight II molecular modeling program (Biosym MSI, San Diego, CA). The Trp-43 in the mutant is generated by replacing His-43 of the F43H/H64L Mb(6) with a tryptophan residue and minimizing the energy of the heme pocket.) The predicted values are similar to the distance between C5 of *d*-camphor and iron in P-450cam. Our earlier studies provided preliminary evidence that Trp-43 in F43W/H64L Mb was oxidatively modified in the reaction with *m*-chloroperbenzoic acid (*m*CPBA), however, the exact structure of the modified product(s) remains to be elucidated.(11) The subject of this study is to identify the oxidized tryptophan residue to determine whether or not the F43W/H64L mutant is capable of performing the oxidation of aromatic molecules.

2. 2 EXPERIMENTAL PROCEDURES

Materials. ^{18}O-labeled *m*CPBA, which was prepared from $^{18}O_2$ as described by Jankowski, S. et al.,(12) was gifted from H. Fujii (associate professor, IMS), and ^{18}O-content of the peroxide was determined to be 72 % by sulfoxidation of thioanisole. $H_2{}^{18}O$ (^{18}O-content 95%) and $^{18}O_2$ (^{18}O-content 98%) were purchased from Icon Services Inc. All other chemicals were purchased from Wako or Nakalai Tesque and used without further purification.

The Oxidation of Trp-43 and the Isolation of Peptide Fragments Bearing Trp-43. F43W/H64L Mb (0.2 mM) in 50 mM potassium phosphate buffer at pH 7.4 was mixed with 4 equivalents of *m*CPBA at 4°C. The modified protein (500 mg) was digested with Lys-C (1/100 w/w) in 100 mM Tris-HCl buffer at pH 9.0 containing 2 M urea, and the mixture was incubated at 25°C for 24 hours. The digestion was stopped by the addition of trifluoroacetic acid (final concentration 1 %). The products were analyzed on an ÄKTA FPLC system (Pharmacia) with a Vydac C-18 reverse phase column eluted typically at a flow of 1.5 mL/min with a gradient of solvent A (0.1% trifluoroacetic acid in water) into solvent B (20 % acetonitrile and 0.1 % trifluoroacetic acid in water) over 200 min. The eluent was monitored either at 280 nm for aromatic residues or 215 nm for amide bonds in peptide fragments. The isolated fragments **A** and **B**, which have been identified as modified Trp-43 linked with unmodified Asp-44–Arg-45–Phe-46–Lys-47 (W*DRFK in which the modified tryptophan is designated as W*), (11) were further treated with trypsin (ca. 1/100 w/w) in 100 mM Tris-HCl buffer (pH 9.0) at 30°C for 12 hours and analyzed by the ÄKTA FPLC system. Although **A** was not cleaved by trypsin, **B** was digested to afford a peptide fragment **B'** (W*DR). In a control experiment, the intact F43W/H64L mutant (250 mg) was treated with Lys-C and trypsin, and the peptide fragment bearing unmodified Trp-43 was isolated by preparative FPLC.

MS/MS Analysis of the Peptide Fragments. The fragments **A** and **B** isolated after Lys-C digestion were directly analyzed on a Voyager DESTR (PerSeptive Biosystems) for MALDI TOF-MS. The spectrometer was calibrated with an angiotensin II (M.W. = 1046.2). 1 μL of the digested samples containing ca. 10 pmol/μL were mixed with 1 μL of saturated α-

cyano-4-hydroxycinnamic acid (CHCA) in water/acetonitrile (1:1) and applied to the sample plate by dried-droplet method.

NMR Spectroscopy. ^{1}H and ^{13}C NMR spectra of **A**, **B'**, and an intact peptide fragment (Trp-43–Asp-44–Arg-45) were obtained either on a UNITY INOVA 600 MHz or on a UNITY puls 600 MHz (VARIAN). ^{1}H and ^{13}C NMR measurements were undertaken in 20 mM potassium phosphate buffer (pD 7.0) in D_2O solution at 25 °C. 3-(Trimethylsilyl)propionic-2,2,3,3-d_4 (TSP-d_4) was used as an internal reference for proton resonances. Complete proton resonance assignments were made using DQF-COSY(13), TOCSY(14,15), and ROESY(16) experiments. The ROE intensities of **A** and **B'** were obtained at 500 ms and 600 ms mixing time, respectively.

Amino Acid Sequence Analysis. Amino acid sequences were analyzed on a Protein Sequencer (Applied Biosystems, model Procise494). The purified intact peptides (WDR) and the modified fragments **A** and **B'** (ca. 10 pmol) were analyzed on a Protein Sequencer (Applied Biosystems, model Procise494) by the Edman method.

Amino Acid Composition Analysis. Amino acid composition was analyzed on a High Speed Amino Acid Analyzer (Hitachi, model L-8500A) to confirm the modification site of **A**. The fragment **A** (2 nmol) was hydrolyzed by heating in 25 μL of 4 M methanesulfonic acid at 110°C for 24 hours. The reaction solution was neutralized with 25 μL of 3.5 M NaOH. The peptide sample was loaded on a High Speed Amino Acid Analyzer (Hitachi, model L-8500 A) with a post-column method.

Determination of Oxygen Source in the Modified Tryptophan. The oxidation of Trp-43 was performed by mixing F43W/H64L Mb with ^{18}O-labeled *m*CPBA in phosphate buffer prepared from $H_2{}^{16}O$ or with [^{16}O]-*m*CPBA in phosphate buffer prepared from $H_2{}^{18}O$. The ^{18}O atom incorporation into modified tryptophan from $^{18}O_2$ was examined by using $^{18}O_2$ (1 atm) saturated phosphate buffer. The oxidation of Trp-43 was performed under Ar gas atmosphere. The modified protein digestion was performed in the presence of Lys-C (1/20 w/w) in 100 mM Tris-HCl (pH 9.0) containing 2 M urea, and the reaction mixture was incubated at 25 °C for 12 hours. The digested products were analyzed on a Vydac C-18 reverse phase column eluted at a flow of 0.4 mL/min with a gradient of solvent A (0.1 %

trifluoroacetic acid in water) into solvent B (20 % acetonitrile and 0.09 % trifluoroacetic acid in water) over 150 min. Peak fractions were collected and analyzed on a SCIEX API 300 (Perkin-Elmer Biosystems) for ESI-MS.

2. 3 RESULTS AND DISCUSSION

The oxidative modification of Trp-43 in F43W/H64L Mb was performed by adding *m*CPBA in 50 mM potassium phosphate buffer at pH 7.4. The transition from 5- to 6-coordinated ferric high spin state is a good indication of the protein modification (**Scheme 1**).(17-21) The *m*CPBA-treated F43W/H64L mutant was digested with Lys-C achromobacter, and two peptide fragments **A** and **B**, which consist of Trp-43(modified)–Asp-44–Arg-45–Phe-46–Lys-47 (W*DRFK), were purified by FPLC. **Figure 2** shows the comparison of the MS/MS spectra of unmodified WDRFK fragment and the modified fragment **A**. The difference in the spectra provides the direct evidence for the modified site to be Trp-43, and the increased mass number of 30 Da could correspond to the addition of two oxygen atoms and loss of two protons. The MS/MS spectrum of the fragment **B** is identical to that of the fragment **A**. Prior to the NMR analysis, **A** and **B** were further treated with trypsin to simplify the NMR spectra. The fragment **B** affords a shorter peptide defined as **B'** (W*DR); however, *trypsin does not cleave the carboxyl side of arginine in the fragment A*. Therefore, we have performed NMR analysis of the intact WDR fragment and modified fragments **A** (W*DRFK) and **B'** (W*DR).

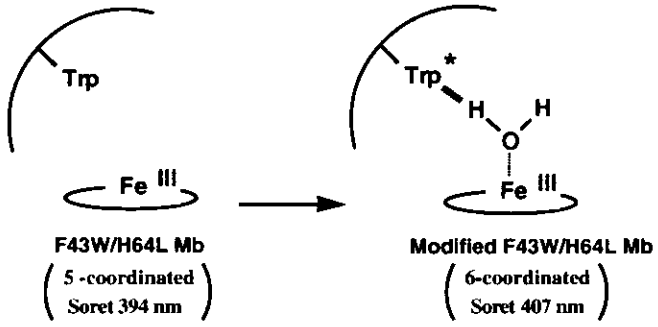

Scheme 1

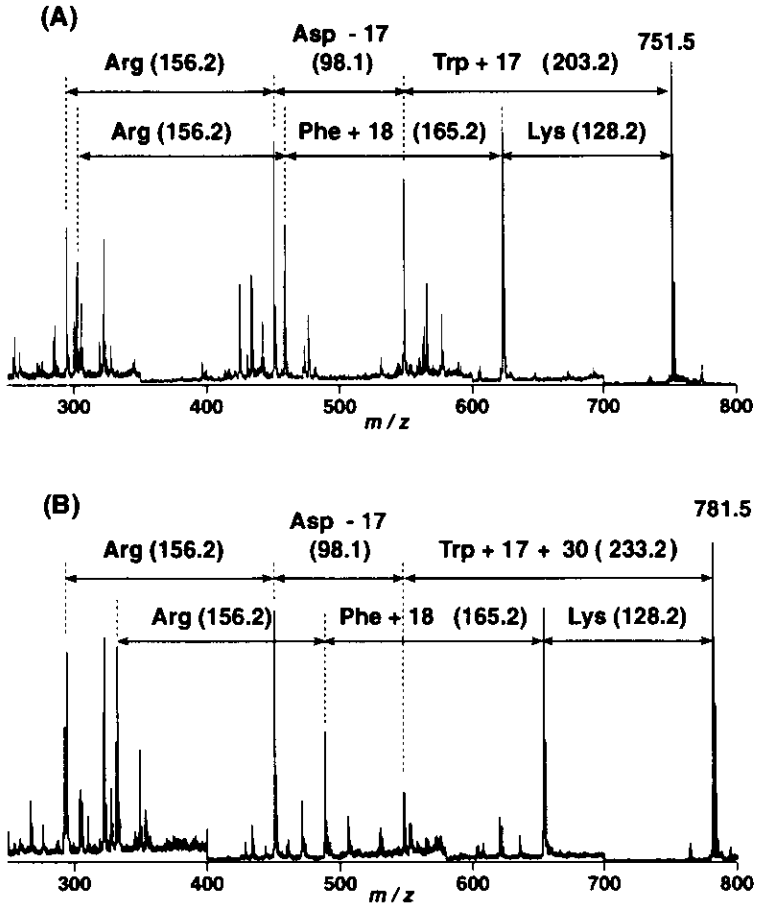

Figure 2. MS/MS analysis of (A) the intact WDRFK fragment and (B) product **A** (W*DRFK) performed on MALDI TOF (PerSeptive Biosystems, Voyager DESTR). The total mass for the intact and modified fragment is 751.5 and 781.5, respectively. Mass units of the major b and y fragment irons are shown. The essentially the same mass pattern was observed for product **B**.

Although the ^{1}H NMR spectrum of the intact WDR fragment exhibits signals derived from five tryptophan protons, only three proton signals of the tryptophan appear in the aromatic region for the modified product **A** (W*DRFK) (**Figure 3, Table 1**). The close examination of the ^{1}H NMR spectrum of **A** reveals that one proton signal at 6.60 ppm couples with two different proton signals with coupling constants of J = 8.2, 2.3 Hz. Two other proton signals appear at 6.58 and 7.19 ppm with coupling constants of J = 2.3 and 8.2 Hz, respectively. The only structure that could afford such a coupling pattern is a 2,6-disubstituted indole substructure as shown in **Figure 4**; i.e., the resonance at 6.58 ppm, 6.60 ppm, and 7.19 ppm are unambiguously assigned to the protons at C7, 5, and 4, respectively.

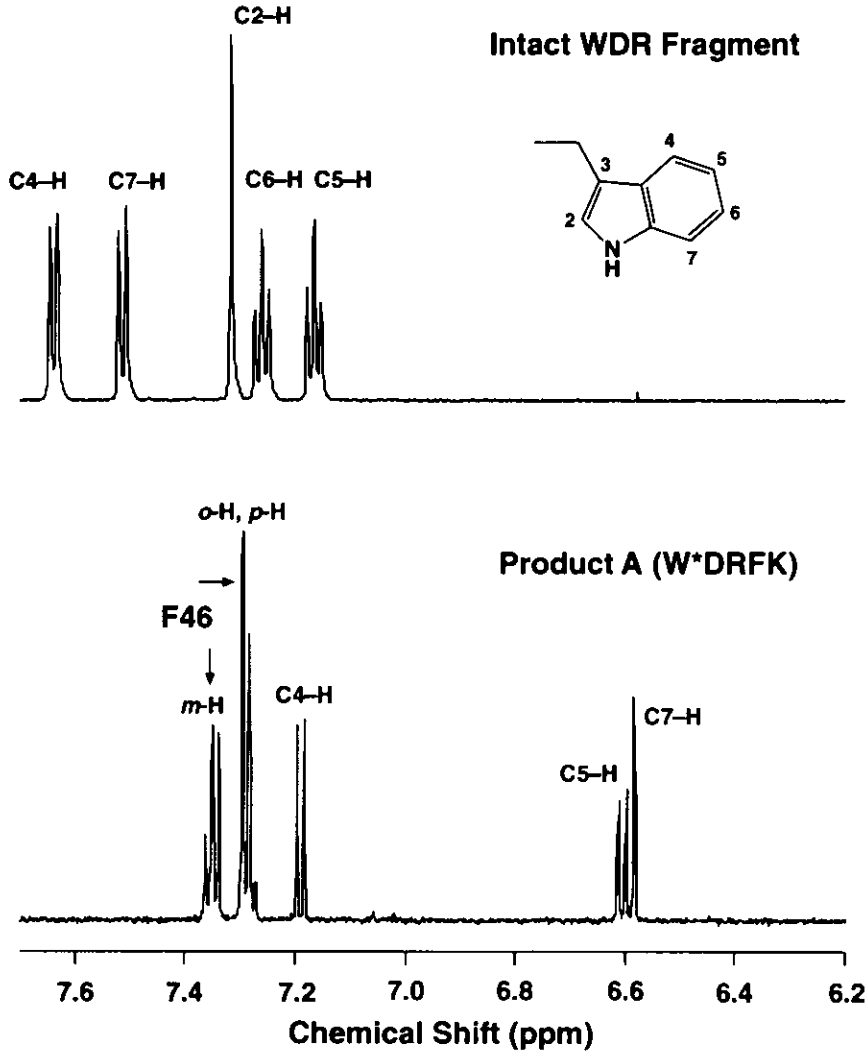

Figure 3 ^{1}H NMR spectra of the unmodified WDR fragment and the modified product **A** (W*DRFK).

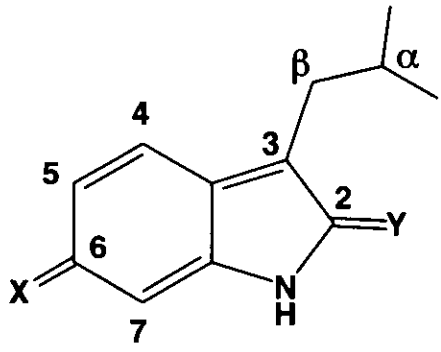

Figure 4 The modified tryptophan structure for both **A** and **B'** on the basis of ^{1}H NMR analysis.

Table 1. ^{1}NMR Chemical Shifts (δ in ppm) of Trp-43 of the intact WDR fragment, product A (W*DRFK), and product B' (W*DR).[a)]

	C^{α}–H	C^{β}–H	C2–H	C4–H	C5–H	C6–H	C7–H
Intact Fragment	**4.35**	**3.46/3.36**	**7.32**	**7.64**	**7.17**	**7.26**	**7.51**
	dd, J=7.0, 7.0	*dd, J=7.0, 7.0*	*s*	*d, J=8.0*	*dd, J=7.2, 8.0*	*dd, J=7.2, 8.0*	*d, J= 8.0*
Product A	**4.14**	**2.65/2.26**	–	**7.19**	**6.60**	–	**6.58**
	dd, J=7.7, 8.7	*dd, J=7.6, 8.9*		*d, J=8.2*	*dd, J=8.2, 2.3*		*d, J= 2.3*
Product B'	**4.46**	**2.90/2.83**	–	**6.91**	**6.26**	–	**6.36**
	dd, J=9.5, 2.9	*dd, J=9.4, 2.9*		*d, J=8.5*	*dd, J=8.5, 2.5*		*d, J= 2.5*

[a)] The NMR spectra were obtained in 20 mM potassium phosphate buffer (pD 7.0) in D_2O at 25 °C on a UNITY INOVA 600 MHz NMR and a UNITY plus 600 MHz spectrometer (Varian). The chemical shifts are referred to TSP-d_4.

The coupling between proton signals at C4 and C5 observed in the COSY spectrum also support the assignment (**Figure 5**). Furthermore, the correlation of the C4–H with C^{α}–H (4.14 ppm) and C^{β}–H (2.65 ppm) was observed by the ROESY experiments (**Figure 6**). The combination of COSY, ROESY, and TOCSY method allows us the complete assignment for the fragment **A** as summarized in **Table 2**. Essentially the same assignment can be applied to the interpretation for the NMR spectra of **B'**. The doublets at 6.36 ppm (J = 2.5 Hz) and 6.91 ppm (J = 8.5 Hz) are assigned to the C7 and C4 protons of the modified Trp-43 in **B'**, respectively. And the resonance at 6.26 ppm (J = 8.5, 2.5 Hz) is derived from C5–H (**Table 1**). Therefore, the tryptophan residue in the fragment **B'** (W*DR) also must have the 2,6-disubstituted indole substructure (**Figure 4**). The coupling pattern in the ^{1}H NMR spectrum of the fragment **B** is essentially the same as those observed in **A** and **B'** spectra.

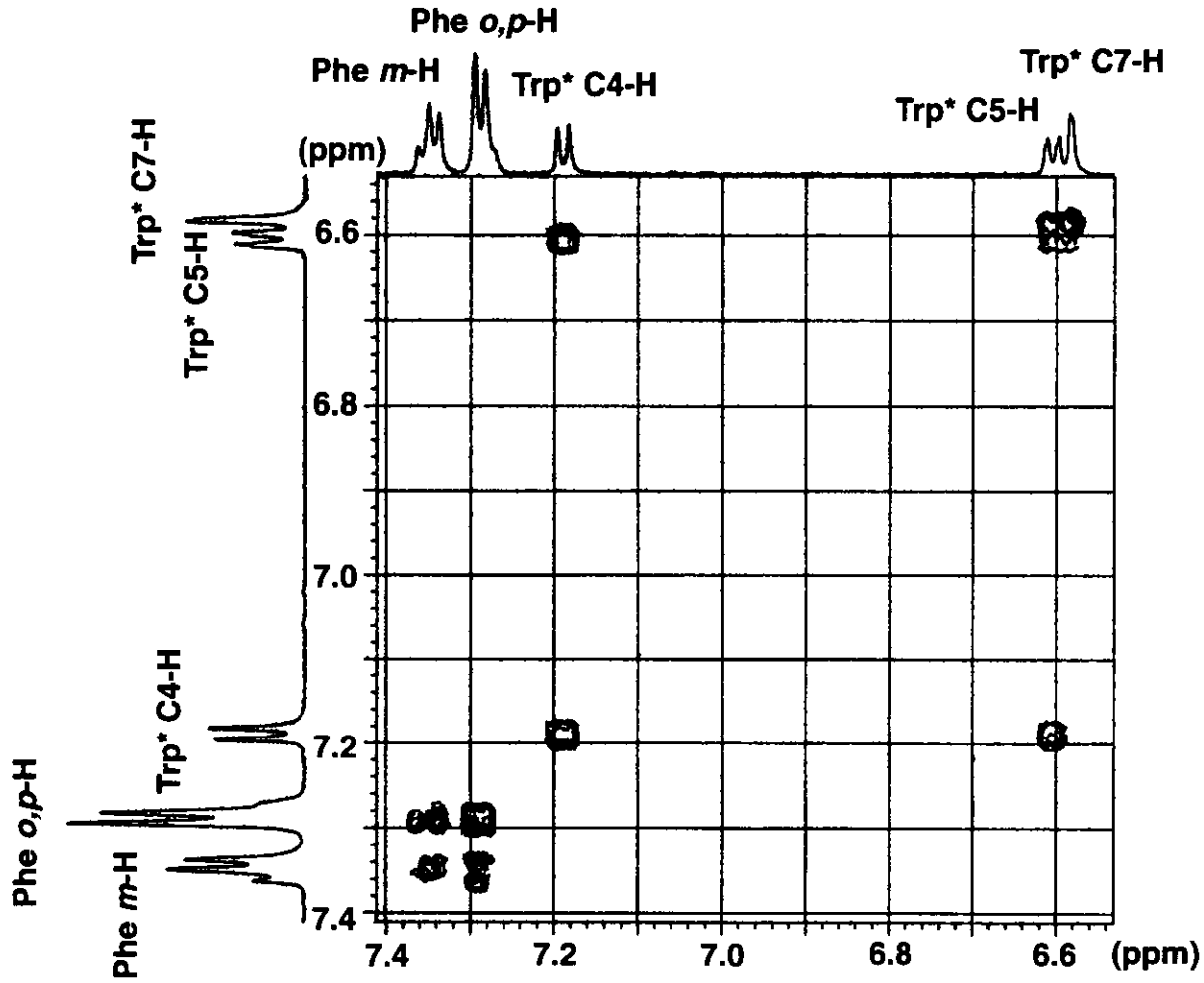

Figure 5. The aromatic region of the 600 MHz COSY spectrum of product A in D_2O at 25 °C

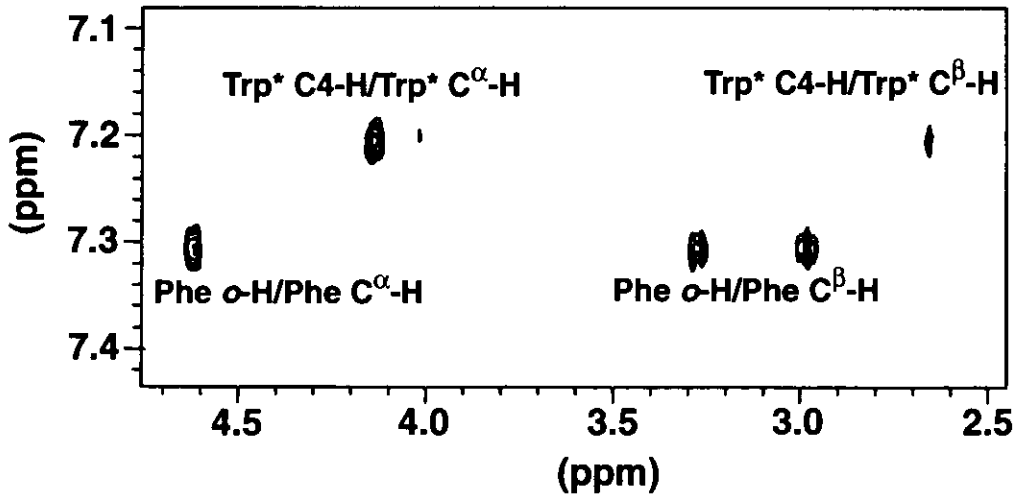

Figure 6. The aromatic region of the 600 MHz ROESY spectrum of product A in D_2O at 25 °C. A 500 msec mixing time was used.

Table 2. ^{1}NMR Chemical Shifts (δ in ppm) for the residues in the intact WDR fragment, product **A** (W*DRFK), and product **B'** (W*DR).[a)]

	C^{α}–H	C^{β}–H	C^{γ}–H	C^{δ}–H	C^{ε}–H	C^{ζ}–H
D in Intact Fragment	**4.69**	**2.77/2.62**				
R in Intact Fragment	**4.10**	**1.80/1.65**	**1.51**	**3.11**		
D in Product A	**4.28**	**2.84/2.60**				
R in Product A	**4.00**	**1.48**	**1.27/1.06**	**3.02**		
F in Product A	**4.61**	**3.26/2.96**		**7.29**	**7.35**	**7.29**
K in Product A	**4.09**	**1.73/1.55**	**1.27**	**1.60**	**2.97**	
D in Product B'	**4.40**	**2.55/2.45**				
R in Product B'	**4.15**	**1.79/1.67**	**1.52**	**3.12**		

[a)] The NMR spectra were obtained in 20 mM potassium phosphate buffer (pD 7.0) in D_2O at 25 °C on a UNITY INOVA 600 MHz NMR and a UNITY PLUS 600 MHz spectrometer (Varian). The chemical shifts are referred to TSP-d_4.

Amino acid sequence and composition analyses provide us with a clue to identify the structural differences in the modified tryptophan of the fragment **A** and **B'**. First of all, **A** does not react with phenylisothiocyanate, and the Edman degradation does not give us any sequence information, while the sequence analysis for **B'** shows Trp*-43(not detected)–Asp-44–Arg-45 sequence. Second, amino acid composition analysis of **A** reveals that the fragment consists of Asp, Arg, Phe, and Lys, however, the modified tryptophan residue has not been clearly identified. The results imply that the amino-terminal of the fragment **A** is protected, but the residues except for Trp-43 are intact. In order to clarify the amino-terminal structure, we have measured ^{13}C NMR of **A** (**Figure 7**). The spectrum exhibits a unique signal at 71.1 ppm, which could be assigned as a signal from the hydroxylated carbon atom. Since the fragment **A** does not contain a serine nor a threonine residue, the comparison of chemical shift for the α carbon in tryptophan (56.1 ppm), indole-3-lactic acid (70.6 ppm), and **A** (71.1 ppm) suggest that the terminal amino group in **A** is replaced with the hydroxyl moiety. Thus, we conclude at the moment that the indole substructure in the modified tryptophan is 2,6-dihydro-2-imino-6-oxoindole in **A** and 2,6-dihydro-2,6-dioxoindole in **B'**. The proposed structures are consistent with the increase in 30 Da mass unit with respect to the intact tryptophan. Unfortunately, we cannot assign chemical shifts of

C2-imino and C6-oxo carbon atoms in product A due to its low concentration.

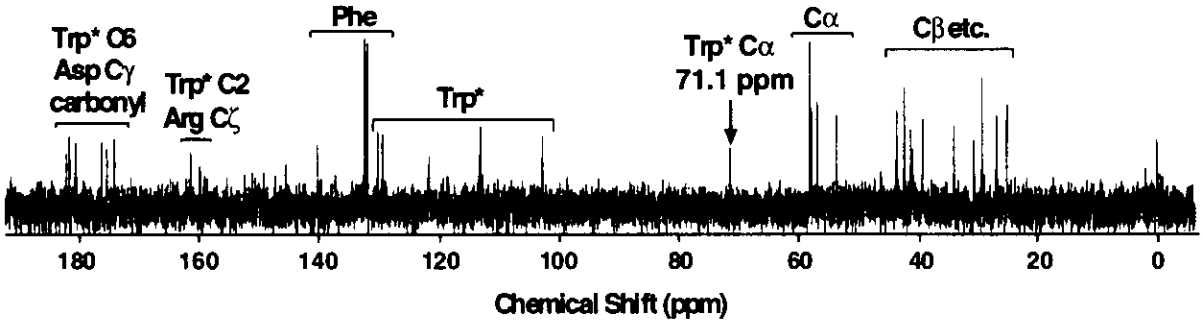

Figure 7. ^{13}C NMR spectrum of product A (W*DRFK). The chemical shifts referred to TSP-d_4.

It should be noticed that trypsin somehow recognizes the structural difference in the amino-terminal of penta-peptide **A** (W*DRFK) and prevents hydrolysis of the carboxyl side of arginine to yield **A'** (W*DR). More interestingly, the fragment **A** is found to be produced from **B** during the incubation with trypsin or Lys-C, while **B** is stable in aqueous solution in the absence of peptidases.

The source of oxygen atoms in modified tryptophan has been examined using ^{18}O-labeled *m*CPBA, H_2O, and O_2 to pursue mechanism of the oxidative modification (**Table 3**). Somewhat interestingly, the results of ^{18}O-incoorporation into product A (2,6-dihydro-2-imino-6-oxoindole) is essentially the same as those for product B (2,6-dihydro-2,6-dioxoindole); therefore, the rearrangement of product B into product A with peptidases does not appear to cause the exchange of oxygen atom at the C2 position. Although further studies are required to clarify the mechanism, 5- or 6-ring intermediate generated through the reaction of the terminal amine with the carbonyl carbon atom at the C2 position followed by hydrolysis might be involved to afford 2,6-dihydro-2-imino-6-oxoindole substructure without changing the total mass of the peptide (**Scheme 2**).

Table 3. Determination of oxygen source in the modified tryptophan.

^{18}O-*m*CPBA (72%)	^{16}O^{16}O (%)	^{16}O^{18}O (%)	^{18}O^{18}O (%)
Product A	**25**	**50**	**25**
Product B	**29**	**49**	**22**
$H_2{}^{18}O$ (91%)			
Product A	**61**	**39**	**0**
Product B	**64**	**36**	**0**
$^{18}O_2$ (98%)			
Product A	**100**	**0**	**0**
Product B	**100**	**0**	**0**

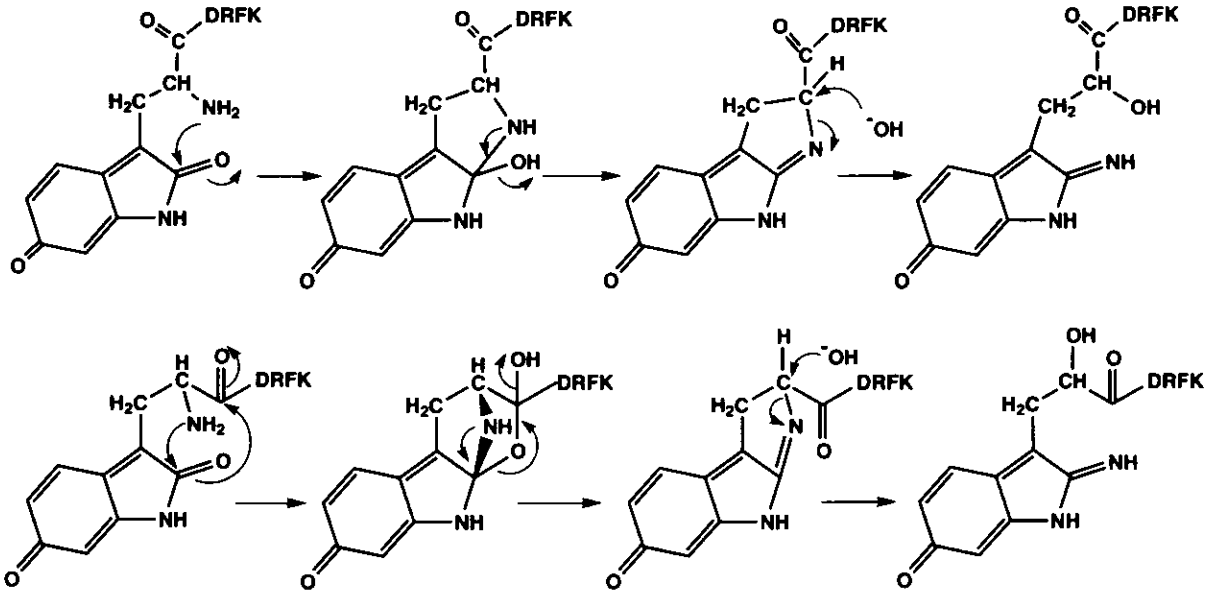

Scheme 2. Possible rearrangement of 2,6-dihydro-2,6-dioxoindole to 2,6-dihydro-2-imino-6-oxoindole.

The ^{18}O-labeling experiments indicate that the oxygen atom of *m*CPBA is incorporated into Trp-43. Since the mixing of *m*CPBA and tryptophan does not produce 2,6-dihydro-2,6-dioxoindole, a ferryl porphyrin radical cation generated in the reaction of F43W/H64L Mb with *m*CPBA is presumably a catalytic species. Previous studies using Fremy's salt as the oxidant indicate that 6-hydroxy-3-methylindole is readily oxidized to yield 3-methylindole 2,6- and 6,7-dione, and 6,7-dione is reported to be a minor product due to its instability (yield

of 3-methylindole 2,6-dione = 63 %, 6,7-dione = 7 %).(22) Therefore, we propose at the moment that C6 or C7 near the heme iron is first oxidized to form 6-hydroxy-tryptophan either directly or via the epoxidation followed by hydrolysis (**Scheme 3**). and then C2 of the 6-hydroxy tryptophan could further be oxidized with *m*CPBA (**Scheme 3A**) or compound I (**Scheme 3B**) by overall four electron oxidation to produce the 2,6-dihydro-2,6-dioxoindole substructure.

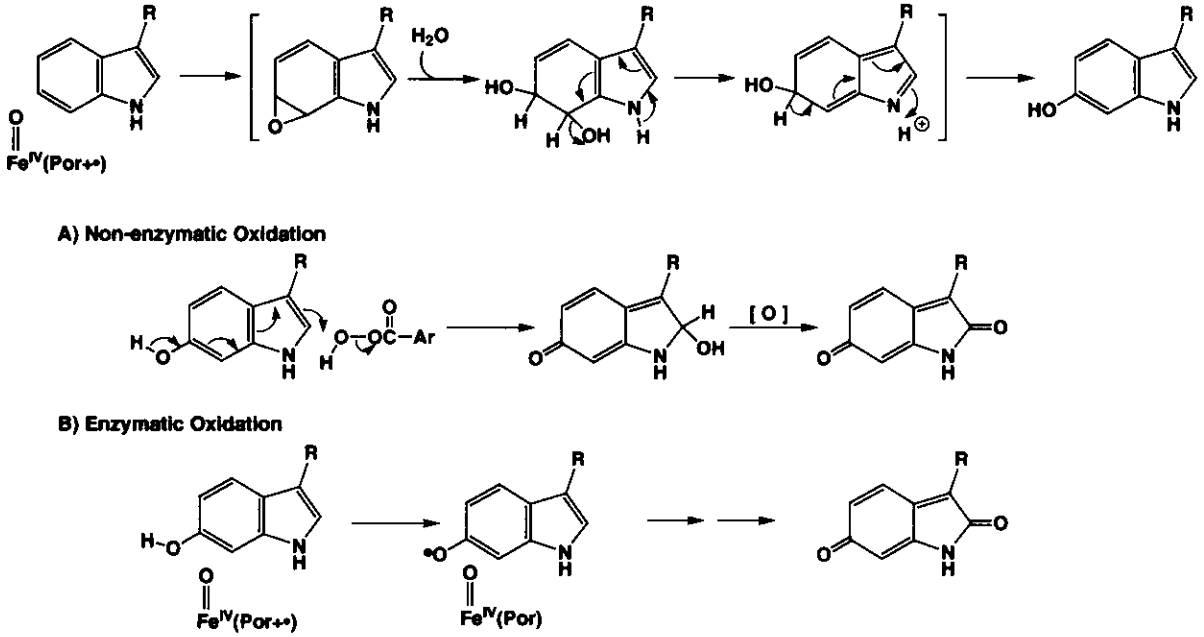

Scheme 3. Plausible mechanisms for the formation of 2,6-dihydro-2,6-dioxoindole.

Since the ^{18}O-labeled product is not generated in $^{18}O_2$, the source of oxygen atoms in modified tryptophan comes from *m*CPBA and H_2O. Furthermore, the double ^{18}O-labeled product is not generated in $H_2{}^{18}O$. If we assume that the hydrolysis of the 6,7-epoxytryptophan is major pass way to yield 6-hydroxy tryptophan, the ^{18}O distribution in tryptophan 2,6-dione in **Table 3** seems to be rationalized.

In summary, we have found that the indole substructure of Trp-43 in F43W/H64L Mb is oxidatively transformed into 2,6-dihydro-2,6-dioxoindole in the presence of *m*CPBA. Our finding is the first example of the oxidation of aromatic carbons by the myoglobin mutant system as far as we know. The results implicate that a ferryl oxygen atom transfer to

aromatic molecules would be possible by a heme enzyme with a non-thiolate ligand if the substrates were fixed nearby the heme iron. Our results would coincide with recent genetic analysis suggesting that a hemoenzyme similar to cytochrome *c* peroxidase with an imidazole as the proximal ligand is involved in biosynthesis of tryptophan tryptophylquinone (TTQ), a novel cofactor bearing indole 6,7-dione moiety, in methylamine dehydrogenase (MADH).(23-25) In addition, we have reported herein that a unique amino-oxo exchange reaction of the *N*-termnal 2,6-dihydro-2,6-dioxoindole performed by Lys-C and trypsin.

2. 4 REFERENCE

1. Adachi, S., Nagano, S., Ishimori, K., Watanabe, Y., Morishima, I., Egawa, T., Kitagawa, T., and Makino, R. (1993) *Biochemistry* **32,** 241-252
2. Rao, S. I., Wilks, A., and Ortiz de Montellano, P. R. (1993) *J. Biol. Chem.* **268,** 803-809
3. Ozaki, S., Matsui, T., Roach, M. P., and Watanabe, Y. (2000) *Coord. Chem. Review* **198,** 39-59
4. Wan, L., Twitchett, M. B., Eltis, L. D., Mauk, A. G., and Smith, M. (1998) *Proc. Natl. Acad. Sci. U.S.A.* **95,** 12825-12831
5. Wittenberg, J., and Wittenberg, B. (1990) *Annu. Rev. Biophys. Biophys. Chem.* **19,** 217-41
6. Ozaki, S., Matsui, T., and Watanabe, Y. (1997) *J. Am. Chem. Soc.* **119,** 6666-6667
7. Ortiz de Montellano, P. R. (1995) in *Cytochrome P450 (2nd Ed)* (Ortiz de Montellano, P. R., ed), pp. 245-303, Plenum Press, New York
8. Watanabe, Y. (1997) in *Oxygenases and model systems* (Funabiki, T., ed), pp. 223-282, Kluwer Academic Publishers, Boston
9. Poulos, T. L., Finzel, B. C., and Howard, A. J. (1987) *J. Mol. Biol.* **195,** 687-700
10. Phillips, G. N. J., Arduini, R. M., Springer, B. A., and Sligar, S. G. (1990) *Proteins: Struct. Funct. Genet.* **7,** 358-365
11. Ozaki, S., Hara, I., Matsui, T., and Watanabe, Y. (2001) *Biochemistry* **40,** 1044-1052
12. Jankowski, S., and Kaminski, R. (1995) *Journal of Labelled Compounds &*

Radiopharmaceuticals **36,** 373-376

13. Piantini, U., Sorensen, O. W., and Ernst, R. R. (1982) *J. Am. Chem. Soc.* **104,** 6800-6801
14. Bax, A., and Davis, D. G. (1985) *J. Magn. Reson.* **65,** 355-360
15. Braunschweiler, L., and Ernst, R. R. (1983) *J. Magn. Reson.* **53,** 521-528
16. Bothnerby, A. A., Stephens, R. L., Lee, J. M., Warren, C. D., and Jeanloz, R. W. (1984) *J. Am. Chem. Soc.* **106,** 811-813
17. Giacometti, G. M., Ascenzi, P., Bolognesi, M., and Brunori, M. (1981) *J. Mol. Biol.* **146,** 363-374
18. Ikeda-Saito, M., Hori, H., Andersson, L. A., Prince, R. C., Pickering, I. J., George, G. N., Sanders, C. R., Lutz, R. S., McKelvey, E. J., and Mattera, R. (1992) *J. Biol. Chem.* **267,** 22843-22852
19. Morikis, D., Champion, P. M., Springer, B. A., Egeberg, K. D., and Sligar, S. G. (1990) *J. Biol. Chem.* **265,** 12143-12145
20. Takano, T. (1977) *J. Mol. Biol.* **110,** 537-568 and 569-584
21. Yonetani, T., and Anni, H. (1987) *J. Biol. Chem.* **262,** 9547-9554
22. Itoh, S., Ogino, M., Haranou, S., Terasaka, T., Ando, T., Komatsu, M., Ohshiro, Y., Fukuzumi, S., Kano, K., Takagi, K., and Ikeda, T. (1995) *J. Am. Chem. Soc.* **117,** 1485-1493
23. Chen, L., Mathews, F. S., Davidson, V. L., Huizinga, E. G., Vellieux, F. S., Duine, J. A., and Hol, W. G. J. (1991) *FEBS Lett.* **287,** 163-166
24. McIntire, W. S., Wemmer, D. E., Chistoserdov, A. E., and Lidstrom, M. E. (1991) *Science* **252,** 817-824
25. Tanizawa, K. (1995) *J. Biochem.* **118,** 671-678

PART III

EFFECTS OF A PHENOLATE AXIAL LIGAND ON THE HEME ENVIRONMENTAL STRUCTURE

ABSTRACT

A double mutant protein of myoglobin (Mb) that exhibits altered axial ligation has been prepared by site-directed mutagenesis. The original axial ligand residue, histidine 93(F8), was replaced with glycine, and also histidine 64(E7) was replaced with tyrosine as an axial ligand, resulting in H64Y/H93G Mb. Tyrosine coordination to the ferric heme iron is verified by optical absorption, EPR and resonance Raman spectroscopy. The optical absorption spectrum of a ferric form of H64Y/H93G Mb is characteristic of high spin heme and similar to those observed in bovine liver catalase and natural occurring mutants of hemoglobin having a phenolate ligand. In contrast, wild-type and H64Y/H93G Mb exhibit almost the same spectra in ferrous and carbon monoxide adduct, suggesting coordination of a histidine residue, possibly histidine 97(FG3), in the reduced forms of the mutant. The phenolate ligation in the ferric H64Y/H93G Mb is confirmed by the observation of $\nu_{Fe\text{-}O}$ band at 597 cm^{-1} in a resonance Raman spectrum. Although EPR spectrum of ferric H64Y/H93G Mb consists of at least two sets of rhombic high spin signals, the major component is similar to bovine liver catalase in the g-values. These results indicate successful conversion of Mb into a catalase-like protein in terms of coordination structure and electronic properties of the heme iron. Regrettably, H64Y/H93G Mb dose not react with H_2O_2, while His-93 $\rightarrow$ Gly mutation gives enough vacant site to accommodate exogenous substrate. Therefore, we conclude that another factor should be required to construct functional model for catalase.

3. 1 INTRODUCTION

The role of the proximal heme iron ligand in activation hydrogen peroxide and control of spin state and coordination number in heme proteins are not yet well understood. Natural heme proteins with protein-derived phenolate ligand are relatively rare. Perhaps the best known natural examples are the tyrosinate-ligated heme-containing catalases, which catalyze the disproportionation of hydrogen peroxide efficiently **(eq. 1 and 2)**. The crystal structures of tetrameric catalases are known **(Figure 1A)**.(1,2) Catalases contain four identical subunits each equipped with a high spin Fe(III)–protoporphyrin IX in the active site. The crystal structure of bovine liver catalase (catalase) shows that a proximal tyrosine (Tyr-357) coordinates to the heme iron, yielding a characteristic five-coordinated ferric heme environmental structure. The distal histidine (His-74) might act as a general acid-base catalyst on the first compound I formation and second H_2O_2 oxidation.(3)

$$\text{Catalase } (Fe^{3+}) + H_2O_2 \longrightarrow \text{Compound I} + H_2O \qquad \text{(eq. 1)}$$

$$\text{Compound I} + H_2O_2 \longrightarrow \text{Catalase } (Fe^{3+}) + O_2 + H_2O \qquad \text{(eq. 2)}$$

Recently it has been found that colal allene oxide synthase, which plays a key role in the conversion of arachidonic acid to prostanoids, has a tyrosinate-ligated five-coordinated ferric heme group.(4,5) Interestingly, colal allene oxide synthase is spectrally similar to catalases, but cannot disproportionate hydrogen peroxide. In addition, a series of naturally occurring hemoglobin (Hb) mutants known as the M Hbs have tyrosinate heme iron ligand.(6-9) Several site-directed mutant heme proteins have been produced with tyrosinate heme iron ligand including various myoglobins,(10-15) and heme oxygense.(16)

The original axial ligand of His-93 in myoglobin (Mb) has been replaced with tyrosine (His-93 → Tyr) by site-directed mutagenesis as a coordination model for catalase **(Figure 1B)**.(10-12) However, the holo-H93Y Mb was obtained after the reconstitution of hemin, which was not suitable as a model for catalase, because tyrosine was larger than histidine. On the other hand, a different approach to coordinating tyrosinate axial ligand has been achieved by His-64 Tyr mutation in Mb **(Figure 1B)**.(13-15) Since the X-ray crystal structure analysis reveals that the polypeptide backbone of the His-64 Tyr Mb is very similar to that of the wild-type protein, the Tyr-64 might be suitable for heme axial ligand in

Mb. But the H64Y Mb is not suitable for catalase model because both of usual axial His-93 and unusual sixth ligand Tyr-64 coordinate to the heme iron, yielding a 6-coordinated ferric heme environmental structure.

To construct 5-coordinated ferric high spin heme with a stable tyrosinate coordination, we have prepared H64Y/H93G Mb **(Figure 1C)**. We expect that the Tyr-64 will coordinate to the heme iron with conserving protein structure, and the H93G mutation gives a space for substrate binding site **(Figure 2)**.(17-22) In addition, His-97 in the H64Y/H93G Mb is placed similar position of distal histidine (His-74) in the catalase **(Figure 3)**. To investigate effects of His-97 on the heme environmental structure, we have prepared H64Y/H93G/H97L Mb and compared with H64Y/H93G Mb.

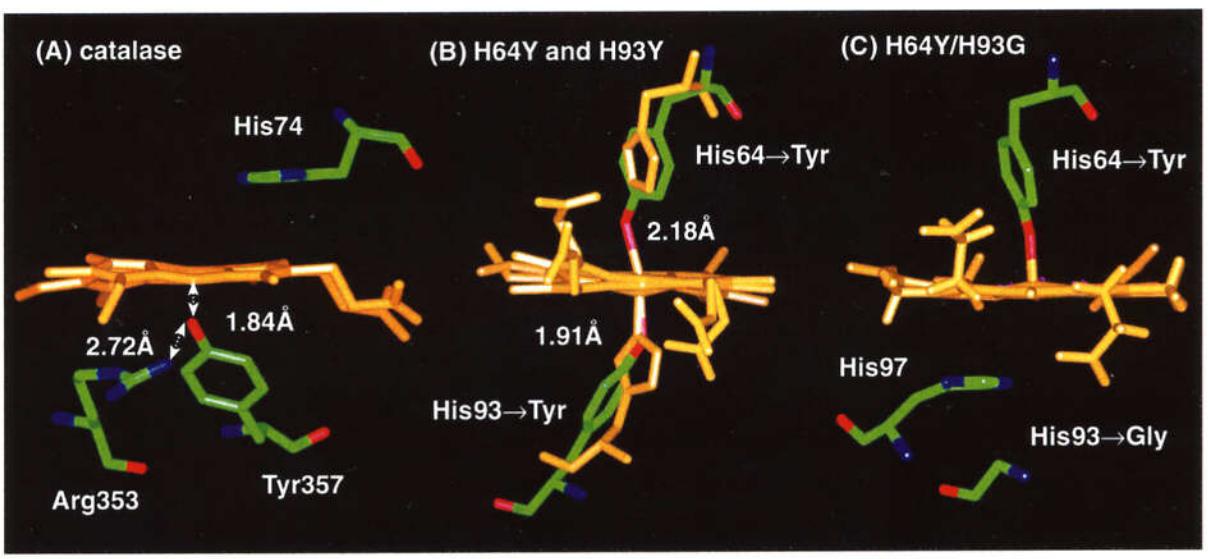

Figure 1. X-ray crystal structure of beef liver catalase (A), superimposed X-ray crystal structures of H64Y and H93Y horse heart myoglobin mutans (B), and calculated structure of H64Y/H93G sperm whale myoglobin (SW Mb) mutant (C) (prepared using InsightII with the H64Y SW Mb structure from the Brookhaven Protein Data Bank).

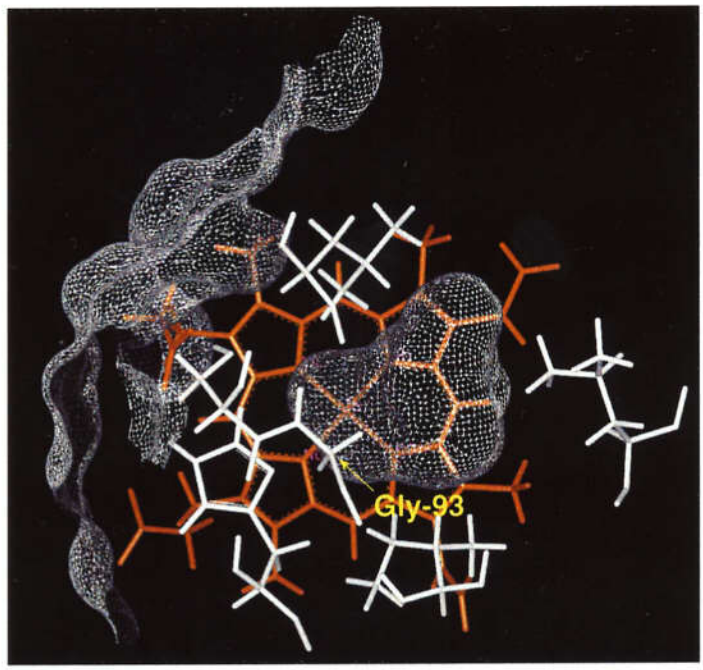

Figure 2. Front sliced view of the active site of H93G Mb with solvent accessible surfaces (white dots) calculated for residues within 8 Å of the heme iron.

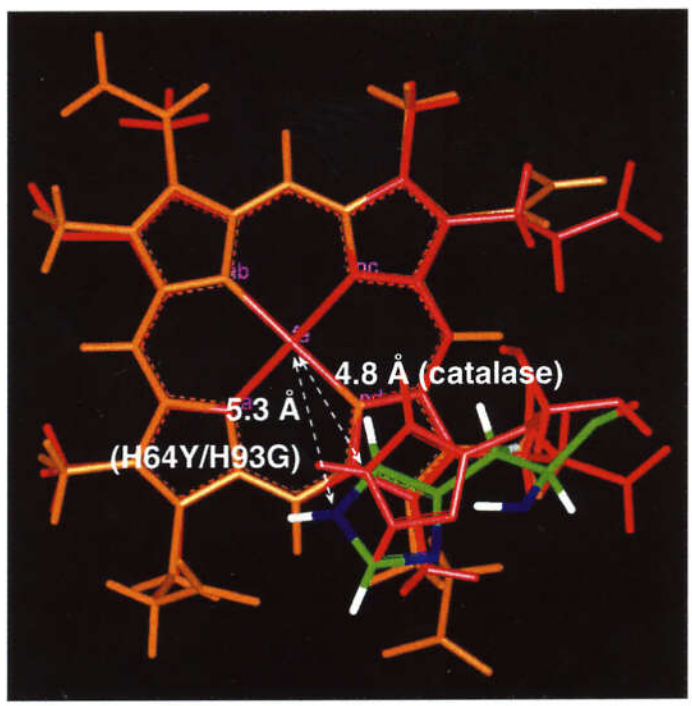

Figure 3. Superimposed structure of catalase shown in red and H64Y/H93G Mb, heme and some selected residues including the distal His-74 in catalase and His-97 in Mb are shown.

3. 2 EXPERIMENTAL PROCEDURES

Materials. Bovine liver catalase (catalase), a thymol-free (C-40, SIGMA), was purified similarly to previous method.(23) The 200 mg of catalase was dissolved in 50 mM Tris-HCl buffer pH 8.0, then absorbed on a anion-exchange column (Resource Q 6 ml, Pharmacia). Proteins were eluted with a buffered linear NaCl gradient to 0.25 M NaCl (total volume, 120 ml). Fractions including catalase in UV spectra were collected and were further purified by size exclusion chromatography (Superdex 75 pg, Pharmacia) with 50 mM potassium phosphate buffer at pH 7.0. The concentration of catalase was determined spectrophotometrically using the value of 3.24×10^5 $M^{-1}cm^{-1}$ for the molar extinction coefficient at 405 nm.(23)

Site-directed Mutagenesis and Protein Purification. The His-93 → Gly and His-97 → Leu mutation were introduced by the polymerase chain reaction (PCR) based method, and the His-64 → Tyr mutation was introduced by the cassette mutagenesis. The expression and purification of the mutants were performed as reported previously.(24,25)

Spectroscopy. The electronic absorption spectra of purified proteins were recorded on a Shimadzu UV-2400 spectrophotometer. The stopped-flow experiments were performed on a Hi-Tech SF-43 equipped with a MG6000 diode array spectrometer.

Titration of the catalase, H64Y/H93G and H63Y/H93G/H97L Mb between pH 2.7 and 9.9 were performed in 50 mM GTA buffer. Each pH was adjusted by adding 5 M NaOH or HCl, and samples were allowed to equilibrate for at least 5 minutes at 4 °C. The titration data were fitted at Soret peak to the Henderson-Hasselbach equation using a Levenberg-Marquardt algorithm.(26)

Resonance Raman spectra of catalase, H64Y/H93G, H63Y/H93G/H97L and H93Y Mb were undertaken in 50 mM phosphate buffer with excitation wavelength at 488.0 nm for ferric forms, at 441.6 nm for ferrous forms, and at 422.6 nm for the carbon monoxide adducts. Typical protein concentrations were 30 μM for Soret excitation and 200 μM for 488.0 nm excitation. Resonance Raman spectra of ferric H64Y/H93G Mb as a function of pH were obtained in 50 mM citrate-potassium phosphate buffer (pH 3.8, 4.4 and 5.0) and potassium phosphate buffer (pH 7.0 and 9.0).

Electron paramagnetic resonance (EPR) spectra of catalase and Mb mutants were recorded on a Bruker ESP-300 instrument operating at 9.5 GHz. Experiments were carried out at microwave power of 1 milliwatt with a field modulation of 1 mT at 100 kHz. An Oxford flow cryostat (ESR-900) was used for liquid helium temperature measurements. Microwave frequency was monitored by a Hewlett-Packard 5350B frequency counter, and a Bruker ER-035M NMR Gauss meter was used to determine the magnetic flux density. All measurements were carried out at 4 K. Concentration of samples were 35 μM for catalase (heme concentration was 140 μM) and 200 μM for Mb mutants.

Reactions with peroxides. The catalase activity of bovine liver catalase, wild type, H64Y/H93G and H63Y/H93G/H97L Mb were measured at 25°C from amounts of molecular oxygen formed on a TD-650 oxygen meter with a Hansantech DW1 oxygen electrode.(27) The reaction mixture typically contained 10 μM Mb and 1 mM H_2O_2 in 50 mM sodium phosphate buffer at pH 7.0. Protein concentration of catalase was used 0.1 μM due to its high activity.

The electronic absorbance changes of H64Y/H93G and H63Y/H93G/H97L Mb (5 μM) upon mixing with either *m*-cloroperbenzoic acid (*m*CPBA) (0.5 mM) or H_2O_2 (1 mM) were measured at 5°C in 50 mM potassium phosphate buffer at pH 7.0. The spectral changes were monitored on a Hi-Tech SF-43 stopped-flow apparatus equipped with a MG6000 diode array spectrophotometer.

3. 3 RESULTS AND DISCUSSION

Electronic absorption spectra of H64Y/H93G, H64Y/H93G/H97L Mb. Figure 4 shows the electronic absorption spectra of ferric, ferrous and carbon monoxide adduct of H64Y/H93G and H64Y/H93G/H97L Mb. The Soret band at 405 nm with broad bands at 492 and 604 nm of ferric H64Y/H93G Mb indicates a typical ferric high-spin heme with tyrosinate coordination (**Figure 4A**). Similar absorption bands in the range of 470-490 nm have observed in the none-heme iron-phenolate proteins and the model compounds and have been assigned to the phenolate-Fe(III) $p\pi$-$d\pi^*$ charge transfer bands.(28-30) The electronic

absorption spectra of ferrous and carbon monoxide adduct of H64Y/H93G Mb are similar to that of wild-type Mb. Ferric spectrum of H64Y/H93G/H97L Mb is identical to the H64Y/H93G Mb, but carbon monoxide adduct of H64Y/H93G/H97L Mb is different from His-Fe(II)-CO form (**Figure 4B**). The result suggests that the His-97 coordinate to ferrous heme of H64Y/H93G Mb as an axial ligand. The His-97 coordination to the ferrous heme iron is also supported by spectral change of Soret peak 416 to 424 nm when imidazole added into the carbon monoxide adduct of H64Y/H93G/H97L Mb (**Figure 5**). The electronic absorption spectra of the ferric forms of catalase, H64Y/H93G and H93Y Mb are shown in **Figure 6**. The Soret peaks of catalase, H64Y/H93G, and H93Y Mb are almost same, but the low energy region of catalase is different from Mb mutants.

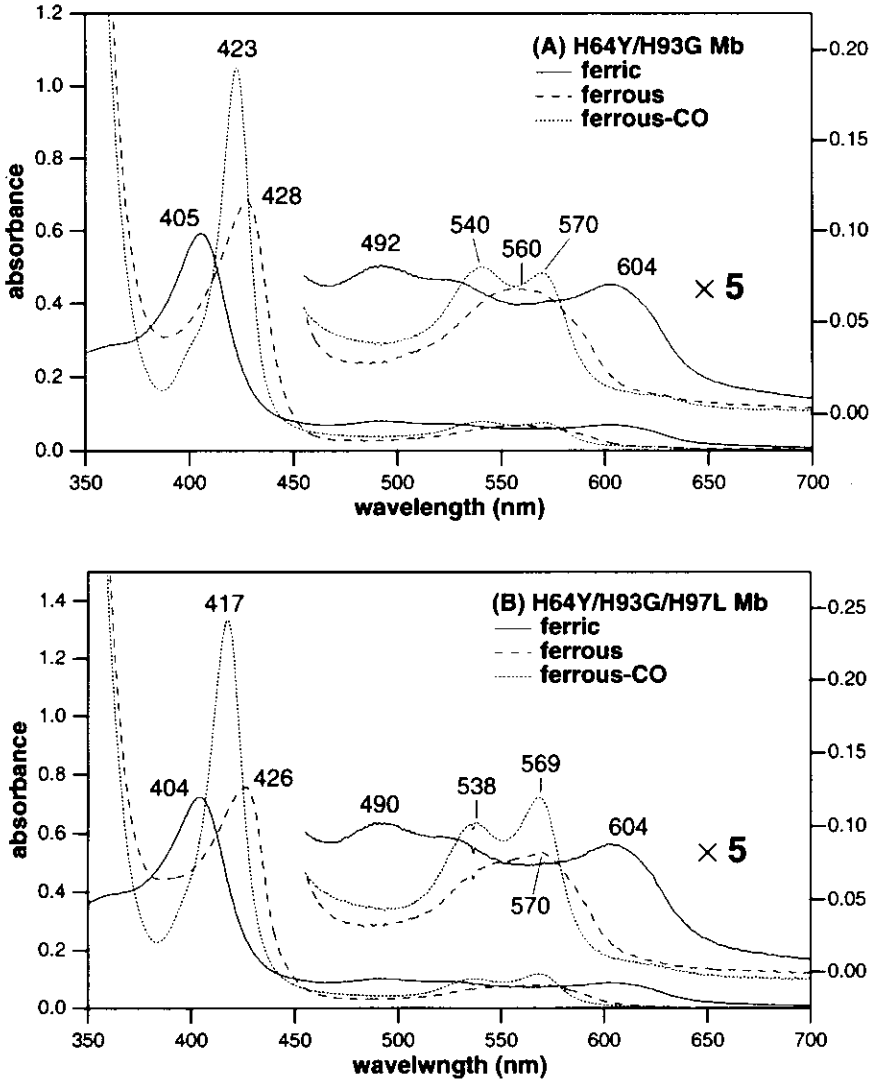

Figure 4. Electronic absorption spectra of ferric (solid line), ferrous (dashed line), and ferrous-CO states (dotted line) for H64Y/H93G and H64Y/H93G/H97L Mb.

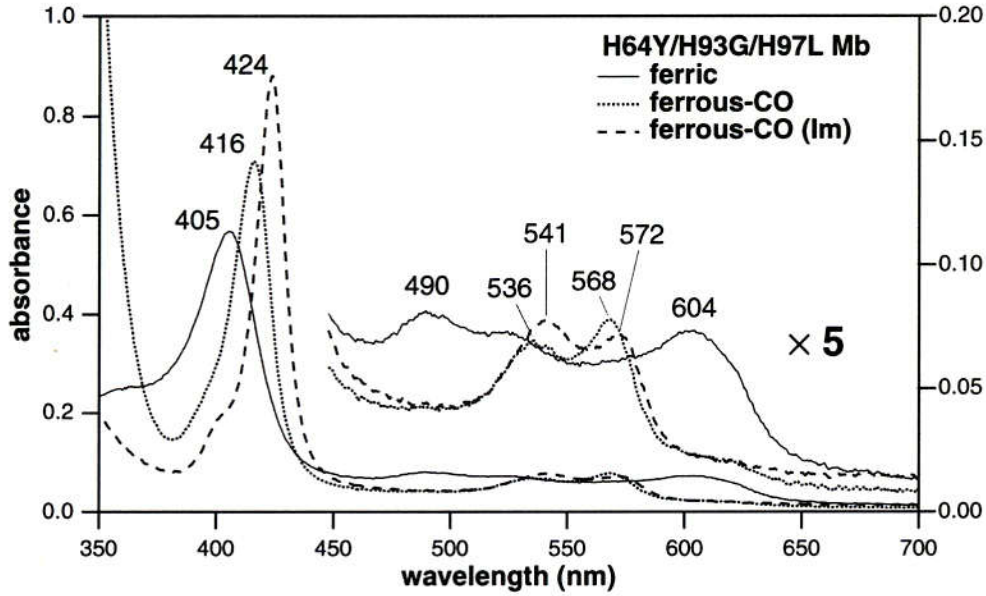

Figure 5. Electronic absorption spectra of ferric (solid line), ferrous-CO (dotted line), and ferrous-CO imidazole (Im) adduct (dashed line) for H64Y/H93G/H97L Mb.

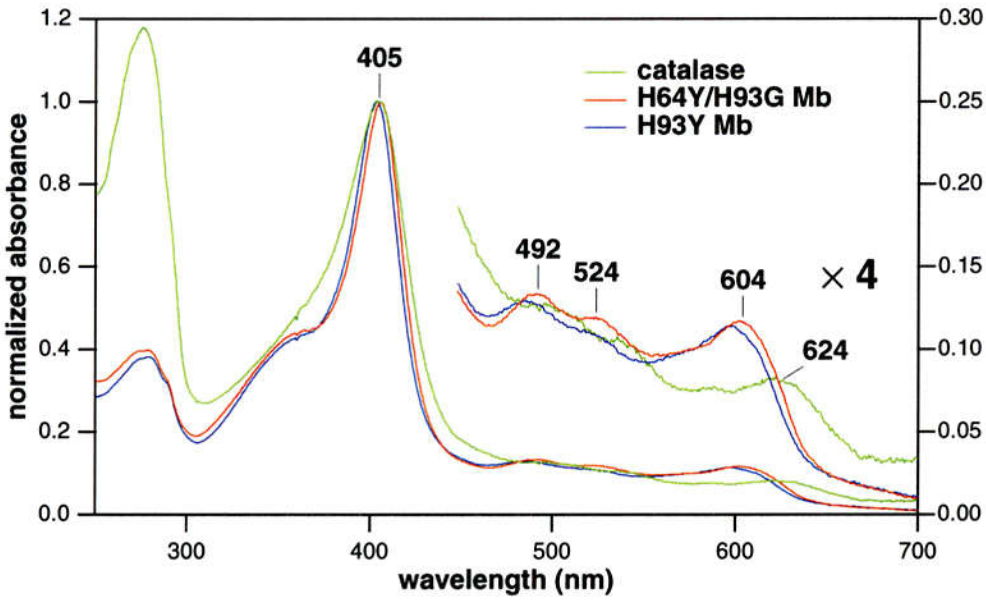

Figure 6. Electtonic absorption spectra of ferric catalase, H64Y/H93G and H93Y sperm whale Mb in 50 mM potassium phosphate buffer at pH 7.0. The spectra are normalized to the absorbance at Soret peak.

Resonance Raman spectroscopy. **Figure 7** shows the resonance Raman spectra of catalase, H64Y/H93G, H64Y/H93G/H97L and H93Y Mbs in ferric form. The high-frequency region reveals bands characteristic of the oxidation state (ν4) and spin and coordination states (ν2, ν3, ν10) of the heme iron atom.(7,31) The ν4 modes appear around 1368-1372 cm^{-1} for ferric state. The ν2, ν3 and ν10 modes of catalase and mutated Mbs have been observed around 1568-1570, 1487-1490 and 1624-1625 cm^{-1}, respectively, and they are characteristic for the 5-coordinate ferric high-spin state.

The Fe-O(Tyr) coordination in H64Y/H93G, H64Y/H93G/H97L and H93Y ferric Mb mutants have been confirmed by the phenolate specific $\nu_{Fe\text{-}O}$ and internal tyrosine modes (**Figure 7, Table 1**).(29) The $\nu_{Fe\text{-}O}$ mode of H64Y/H93G and H64Y/H93G/H97L Mb mutants are observed at 597 cm^{-1}, and those are shifted +14 cm^{-1} from the $\nu_{Fe\text{-}O}$ mode of H93Y Mb (583 cm^{-1}). The another four internal tyrosine modes, phenolate C-O stretching mode ($\nu_{Tyr(C\text{-}O)}$) and three phenolate ring modes ($\nu_{Tyr(C=C)}$×2 and $\delta_{Tyr(C\text{-}H)}$), of H64Y/H93G and H64Y/H93G/H97L Mb mutants are observed arround at 1281 cm^{-1}, 1500-1501 cm^{-1}, 1624-1626 cm^{-1} and 1166-1167 cm^{-1}, respectively. Although the three phenolate ring modes are similar to the H93Y Mb (1502 cm-1, 1604 cm^{-1} and 1169 cm^{-1}), the $\nu_{Tyr(C\text{-}O)}$ are shifted –9 cm^{-1} from the H93Y Mb (1300 cm^{-1}). This result together with the up shift of $\nu_{Fe\text{-}O}$ indicates greater donation of electrons from phenolate to the heme iron for H64Y/H93G and H64Y/H93G/H97L Mb mutants. Additionally, it has been shown that the His97 →Leu mutation does not affect the iron-tyrosine bond.

Although the crystallographic studies showed the proximal ligand in catalases to be a tyrosine,(1,2) the tyrosine-iron coordination bands are not detectable expect for the phenolate ring mode (1612 cm^{-1}) in **Table 1**.(32,33) On the other hand, the tyrosine-iron coordination of H64Y/H93G and H64Y/H93G/H97L Mb mutants are similar to the Hb M Boston (His-E7(58)α →Tyr) in the Raman frequency (1603, 1505, 1279 and 603 cm^{-1} in **Table 1**)(7) which has the tyrosine coordinated heme iron with displacing the usual proximal histidine, yielding a five-coordinated iron structure.(34)

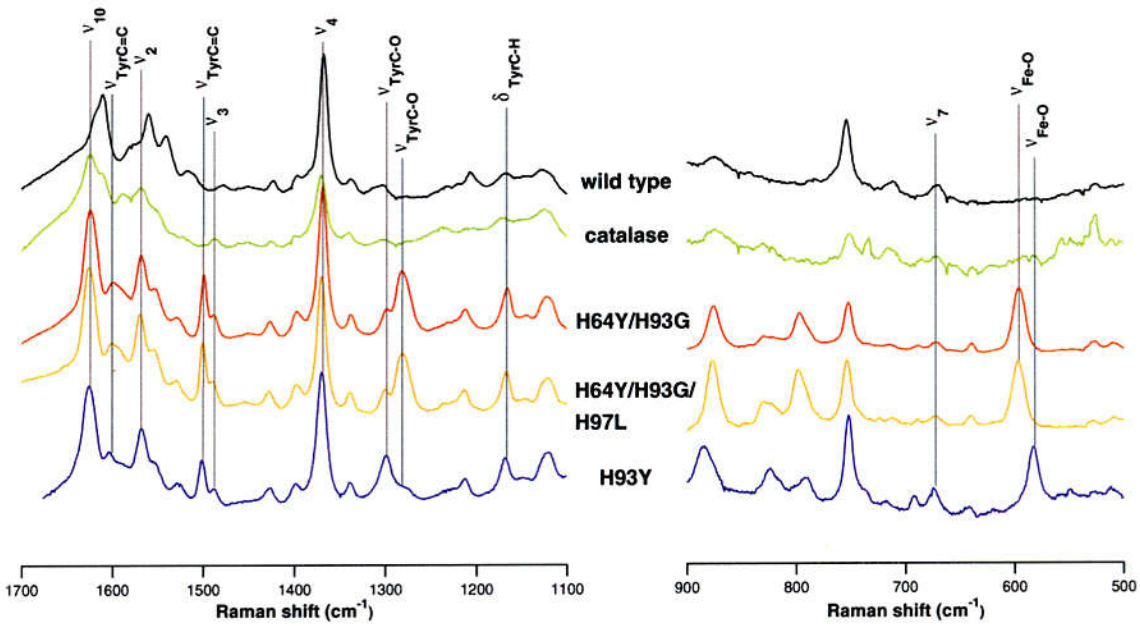

Figure 7. Resonance Raman spectra of ferric form of wild type Mb, catalase, H64Y/H93G, H64Y/H93G/H97L and H93Y Mb in 50 mM potassium phosphate buffer pH 7.0. The laser excitation wavelength is 488 nm. Heme concentration is 200 μM for WT Mb and its mutants and is 140 μM for catalase.

Table 1. Resonance Raman frequencies of catalase, Mbs and Hb M Boston in ferric form.

	Bovine liver catalase	H64Y/H93G	H64Y/H93G/ H97L	H93Y	Hb M Boston[a]	Wild Type Mb
ν_{Fe-O}	ND[b]	597	597	583	603	none
$\nu 7$	672	672	673	674	677	670
$\delta_{Tyr(C-H)}$	ND	1166	1167	1169	–	none
$\nu_{Tyr(C-O)}$	ND	1281	1281	1300	1279	none
$\nu 4$	1370	1369	1370	1370	1372	1368
$\nu 3$	1487	1489	1490	1489	1490	1478
$\nu_{Tyr(C=C)}$	ND	1500	1501	1502	1505	none
$\nu 2$	1568	1568	1570	1568	1573	1560
$\nu_{Tyr(C=C)}$	1612[c]	1600	1600	1604	1603	none
$\nu 10$	1625	1624	1626	1625	1628	1611

(a) Nagai et al. 1983, 1989.

(b) not determined

(c) Assignment based on Sharma et al. 1989.

Figure 8A shows the resonance Raman spectra of wild type and H64Y/H93G Mb in ferrous form. H64Y/H93G Mb exhibits the $\nu_{Fe\text{-}His}$ band at 220 cm^{-1} identical to the wild type with weak intensity, which suggests weak ligation of His-97 to the ferrous heme iron. **Figure 8B** presents the Raman spectra of wild type, H64Y/H93G, and H64Y/H93G/H97L Mb in carbon monoxide adduct. The $\nu_{Fe\text{-}CO}$ vibration is observed at 505 cm^{-1} in wild type Mb. On the other hand, H64Y/H93G/H97L Mb exhibits two different $\nu_{Fe\text{-}CO}$ modes at 520 and 488 cm^{-1}. H64Y/H93G/H97L Mb dose not have histidine around heme iron, and it is unlikely that ferrous iron is bounded to the phenolate group of tyrosine. Although further studies are required to clarify the exact structures of CO-bounded forms for H64Y/H93G/H97L Mb, two different $\nu_{Fe\text{-}CO}$ modes could be derived from CO binding on the distal or proximal side of ferrous heme with water molecule on the other side. The $\nu_{Fe\text{-}CO}$ band at 488 cm^{-1} in H64Y/H93G Mb indicates His-97 ligated CO form. It should be noticed that the $\nu_{Fe\text{-}CO}$ band at 520 cm^{-1} also observed for minor component in H64Y/H93G Mb. This implicates that Fe-His bond is partially dissociated because of the weak ligation.

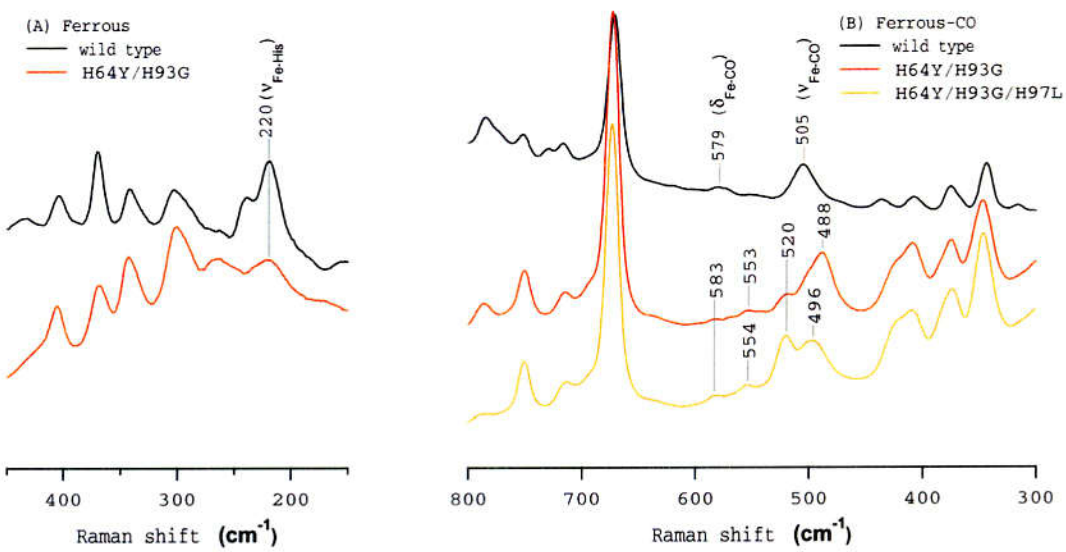

Figure 8. Resonance Raman spectra of ferrous form of wild type and H64Y/H93G Mb (A), and ferrous-CO form of wild type, H64Y/H93G, and H64Y/H93G/H97L Mb (B) in potassium phosphate buffer at pH 7.0. The laser excitation wavelength is 441.6 nm for ferrous form and 422.6 nm for ferrous-CO form. Heme concentration is 200 μM for 488.0 nm excitation and 30 μM for 422.6 nm excitation.

Electron paramagnetic resonance (EPR) spectroscopy. The EPR spectra of catalase, H64Y/H93G, H64Y/H93G/H97L and H93Y Mb in 50 mM potassium phosphate buffer at pH 7.0 indicate high-spin ferric state with rhombically split signals in the ~ g=6 region (**Figure 9**). The catalase exhibited g values of g_x=6.46, g_y=5.34 and g_z=1.98. The EPR spectrum of H64Y/H93G Mb exhibits at least two sets of rhombic high spin signals, the major component (g_x=6.57) is similar to catalase in g values. This result indicates successful conversion of Mb into a catalase-like protein in terms of electronic properties of the heme iron. On the other hand, H64Y/H93G/H97L Mb exhibits narrow rhombic signal in the major component (g_x=6.27). Since the His-97 ring is fixed near by heme, the difference in g value could arise from perturbation of the heme symmetry. More importantly the H64Y/H93G and H64Y/H93G/H97L Mb mutants lack a g=6 signal which indicates an axial symmetric high spin species observed in H93Y Mb. This implicates stable iron-tyrosine coordination for H64Y/H93G and H64Y/H93G/H97L Mb mutants.

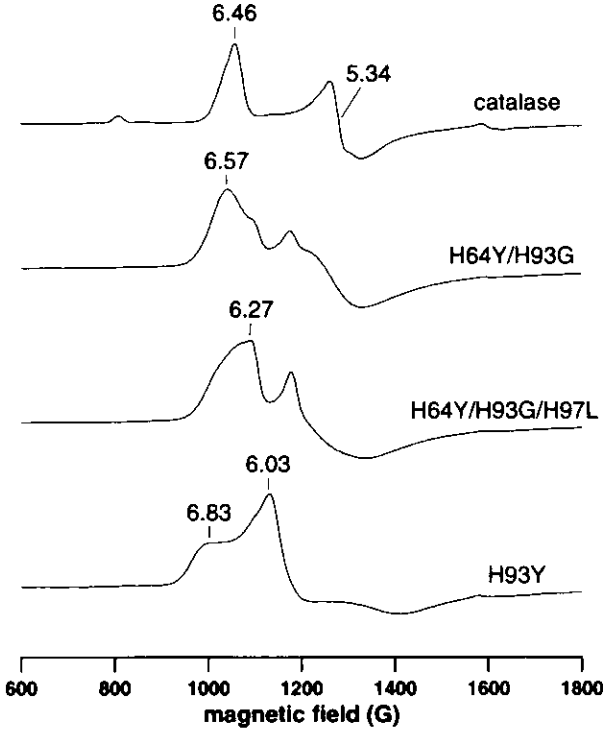

Figure 9. EPR spectra of ferric form of catalase, H64Y/H93G, H64Y/H93G/H97L and H93Y Mb. EPR conditions: concentration 200 μM (Mb mutants) and 140 μM (catalase) in 50 mM potassium phosphate buffer at pH 7.0, modulation frequency 100 kHz, modulation amplitude 7.6 G, power 1 mW, temperature 4 K.

Reaction of H64Y/H93G and H64Y/H93G/H97L Mb mutants with peroxides. The dismutation of hydrogen peroxide has been examined for catalase, wild type Mb, H64Y/H93G and H64Y/H93G/H97L Mb mutants (**Table 2**).(27) A molecular oxygen is not produced during the reaction of H64Y/H93G and H64Y/H93G/H97L Mb mutants with hydrogen peroxide. The ferric heme of wild type Mb is oxidized by hydrogen peroxide to a ferryl heme (Fe^{IV}=O Por) equivalent to compound II of peroxidase,(35-37) however, no spectral changes have been observed during reaction of H64Y/H93G and H64Y/H93G/H97L Mb mutants with hydrogen peroxide. These results suggest that ferric heme of H64Y/H93G and H64Y/H93G/H97L Mb mutants can not react with hydrogen peroxide, because anionic phenolate ligand neutralizes positive charge of ferric heme with reducing its Lewis acidity. On the contrary, heme degradation has been observed in H64Y/H93G and H64Y/H93G/H97L Mb mutants upon mixing with *m*-chloroperbenzoic acid (*m*CPBA) (**Figure 10**). Since the His-93 → Gly mutation gives a large space for substrate binding site,(17-22) vacant site of H64Y/H93G Mb is able to accommodate *m*CPBA.

Table 2. Reaction of catalase, wild type and its mutants with H_2O_2.

Protein	Oxygen evolution[a] (turnover/min)
Catalase	3790
Wild type	1.7
H64Y/H93G	0
H64Y/H93G/97L	0

[a]H_2O_2 (1 mM) was added to a reaction mixture containing Mb (10 μM) in 50 mM sodium phosphate buffer (pH 7) at 25 °C. Protein concentration of catalase was used 0.1 μM due to its high activity.

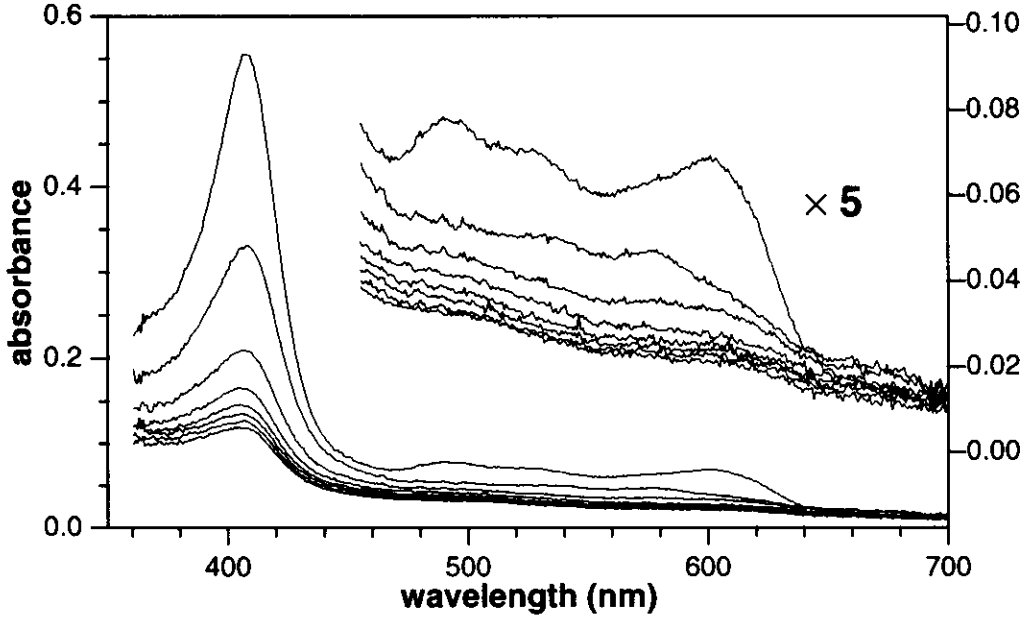

Figure 10. Absorption spectral changes of H64Y/H93G Mb (5 mM) upon mixing with *m*CPBA (0.5 mM) at 5°C in 50 mM potassium phosphate buffer at pH 7.0. The spectra taken every 12 msec are shown.

pH titrations. The absorption spectra of the catalase, H64Y/H93G, and H64Y/H93G/H97L Mb mutants as a function of pH are shown in **Figure 11**. H64Y/H93G Mb exhibits no spectra change between pH 10 and 5, and the blue shift of the Soret peak at 405 nm to 375 nm has been observed at pH less than 5. Since the absorption maximum of CT band at 600 nm also shifted to 640 nm at pH less than 5, the Soret peak decreasing in intensity indicates that the heme iron-tyrosine bond is disrupted at low pH. The pK_a value of heme iron-tyrosine bond disruption is found to be 4.3 for H64Y/H93G Mb. The H64Y/H93G/H97L Mb exhibits similar spectral change to H64Y/H93G Mb with pK_a value of 4.4. These pK_a values are ca. 1 pH unit lower than the value of 5.6 determined for the H64Y Mb,(14) which exhibits 6-coordinate ferric heme structure with Tyr-64 and His-93 as axial ligands. On the other hand, catalase exhibits pK_a value of 3.6 that is ca. 1 pH unit lower than the values of H64Y/H93G and H64Y/H93G/H97L Mb mutants. This result suggests that the presence of hydrogen bonding between Tyr-357 phenol oxygen and Arg-353 ζ nitrogens may decrease the potential of deprotonation of the phenol oxygen.

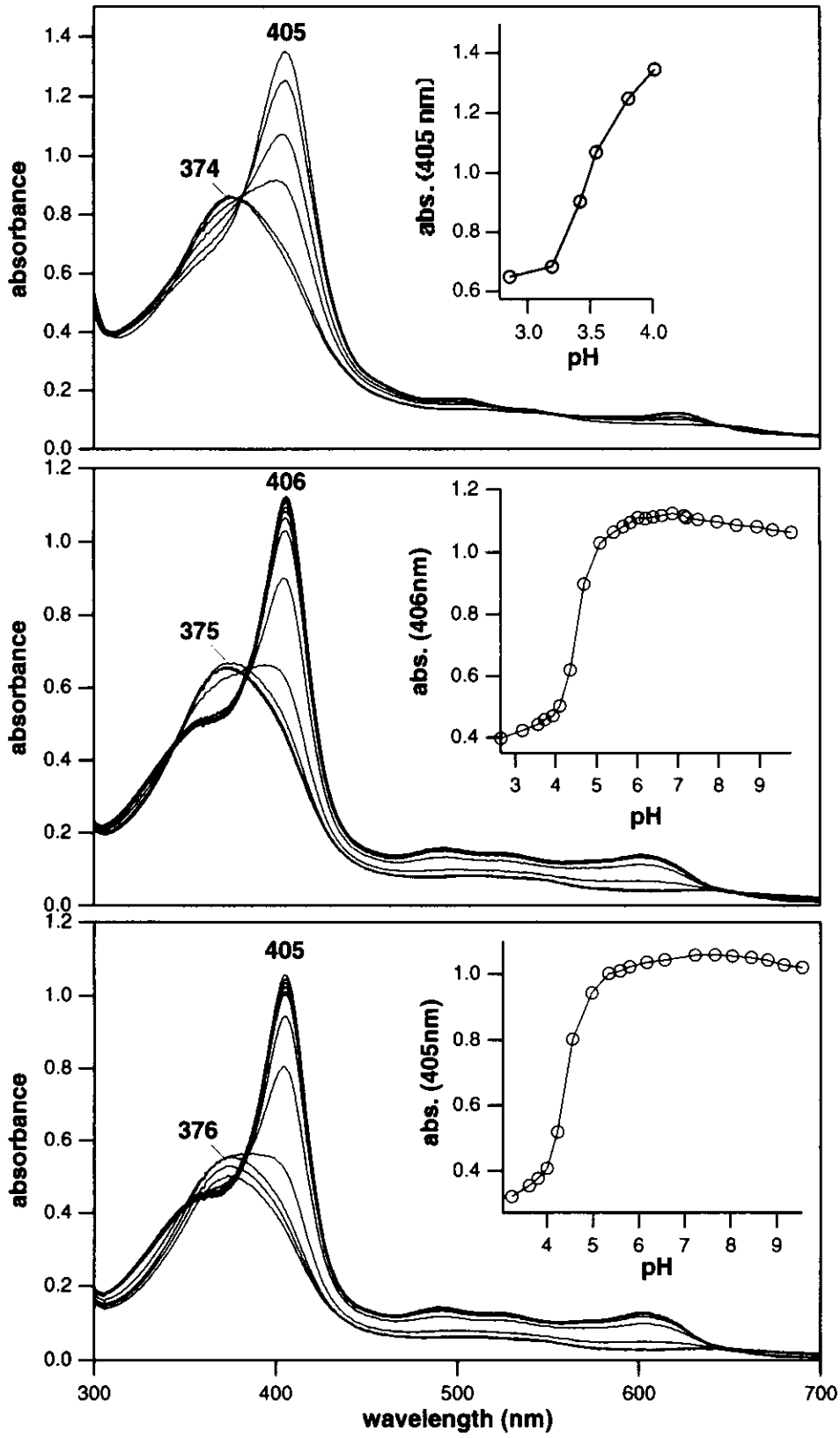

Figure 11. Absorption spectra of catalase (A), H64Y/H93G (B) and H64Y/H93G/H97L (C) SW Mb as a function of pH. Insets indicate the titration curve based on a Soret maximum absorption band. The titration data were fit to the Henderson-Hasselbach equation using a Levenberg-Marquardt algorithm.

The resonance Raman spectra of H64Y/H93G Mb between pH 9.0 and 3.8 are shown in **Figure 12**. The resonance Raman bands of ferric heme iron-tyrosine ($\nu_{Fe\text{-}O}$, $\nu_{Tyr(C=C)}\times 2$ and $\delta_{Tyr(C\text{-}H)}$) disappear at pH 3.8. This result clearly exhibits that the ferric heme iron-tyrosine bond was disrupted at pH 3.8. Since the heme maker bands are not altered even at pH 3.8, the 5-coordinate structure is conserved with another ligand presumably a water molecule.(38,39)

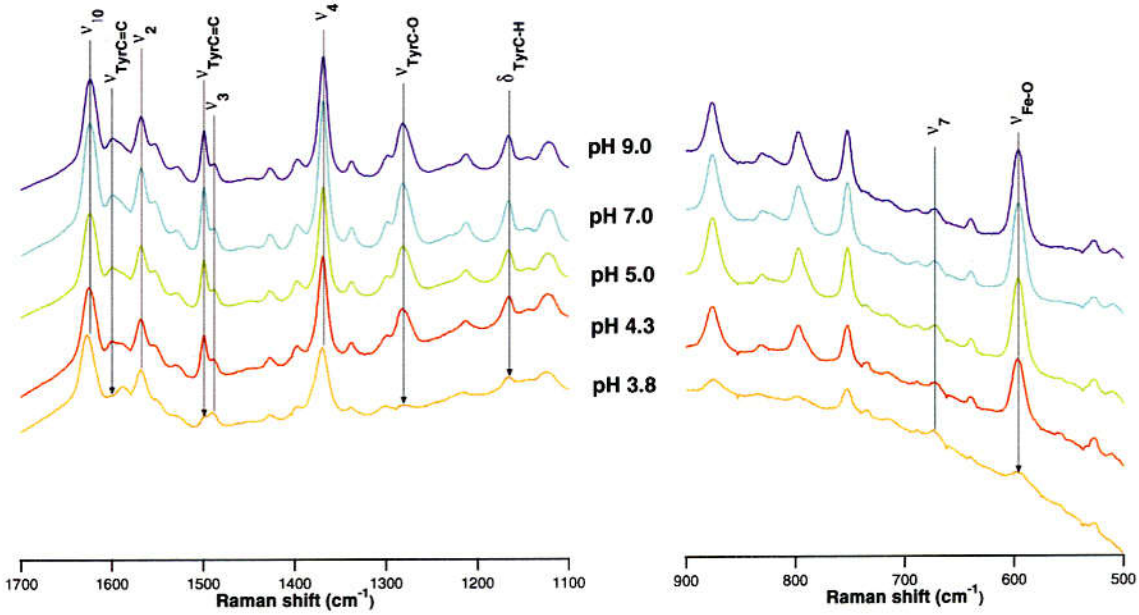

Figure 12. Resonance Raman spectra of H64Y/H93G Mb at different pH value excited at 488.0nm. Buffers used are 50mM citrate-potassium phosphate for pH3.8-5.0 and potassium phosphate for pH7.0-9.0. Heme concentration is 200 μM.

The effects of pH on the EPR spectra of catalase and H64Y/H93G Mb are obtained between pH 9 and 3.0 (**Figure 13**). A new axial signal grows at g=6 as disruption of iron-tyrosine bond at low pH. The two sets of rhombic signals of H64Y/H93G Mb exhibit no pH dependence in the range of pH 9.0-5.0. On the other hand, two major rhombic high-spin signals have been observed during the pH titration of catalase. The narrow rhombic signal is dominant above pH 7.0, and broad rhombic signal is observed below pH 4.0. It has been known that the similar spectra change is taken place in 30% (v/v) glycerol solution with pK_a value of 6.0.(40) Since the pK_a value is identical to that of histidine side chain, protonation of histidine in heme vicinity may effect on the local heme symmetry. This implicates the

His-97 in H64Y/H93G Mb may not act as a general acid base catalyst, because of the hydrogen bonding with the 7-propionate carboxylate.

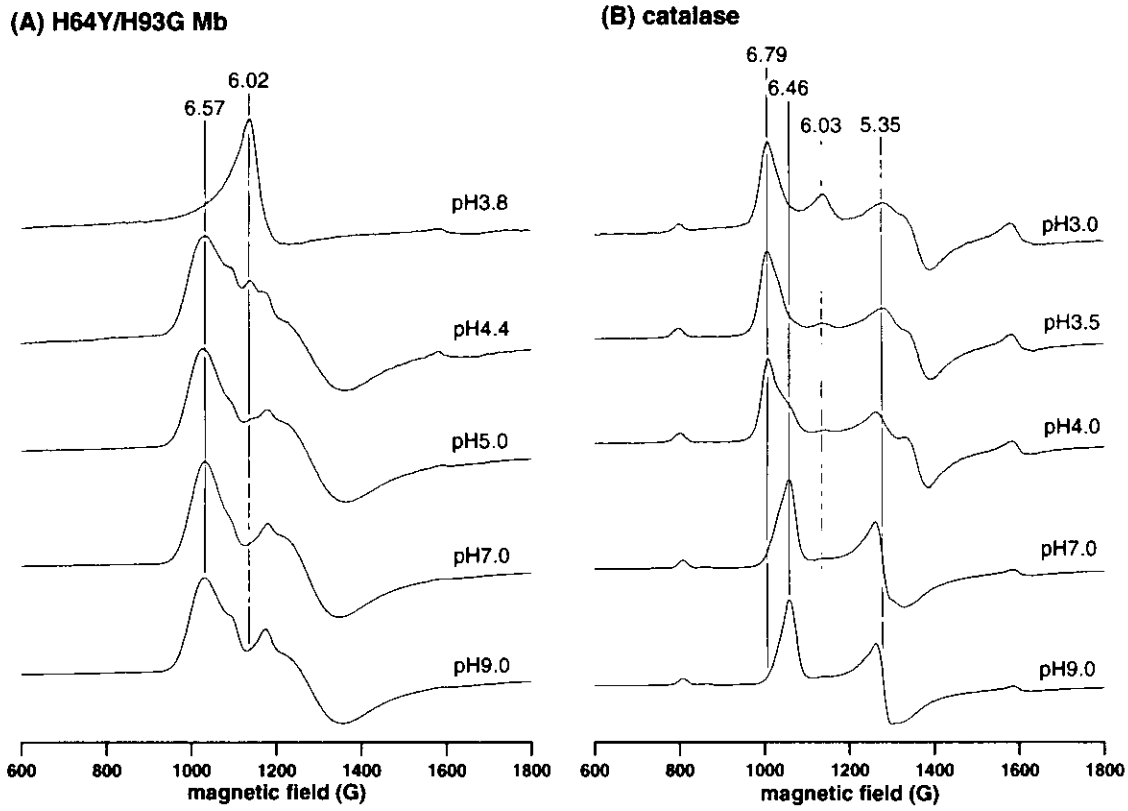

Figure 13. EPR spectra of H64Y/H93G Mb (A) and catalase (B) at different pH values. EPR conditions: concentration 200 μM (Mb mutants) and 140 μM (catalase) in 50 mM citrate-potassium phosphate buffer (pH 3.8, 4.4 and 5.0) and potassium phosphate buffer (pH 7.0 and 9.0), modulation frequency 100 kHz, modulation amplitude 7.6 G, power 1 mW, temperature 4 K.

In summary, the double mutation of the distal His-64 → Tyr and the proximal His-93 → Gly achieves successful conversion of Mb into catalase like protein in terms of coordination structure and electronic properties of ferric heme iron. The His-97 in the H64Y/H93G Mb, which is fixed same position of distal histidine in catalase, contribute to construct catalase like heme symmetry. Regrettably, H64Y/H93G Mb dose not react with H_2O_2, while His-93 → Gly mutation gives enough vacant site to accommodate exogenous substrate. Therefore, we conclude that another factor should be required to construct functional model for catalase.

3. 4 REFERENCE

1. Murthy, M. R. N., Reid, T. J., Sicignano, A., Tanaka, N., and Rossmann, M. G. (1981) *J. Mol. Biol.* **152,** 465-499
2. Vainshtein, B. K., Melikadamyan, W. R., Barynin, V. V., Vagin, A. A., Grebenko, A. I., Borisov, V. V., Bartels, K. S., Fita, I., and Rossmann, M. G. (1986) *J. Mol. Biol.* **188,** 49-61
3. Putnam, C. D., Arvai, A. S., Bourne, Y., and Tainer, J. A. (2000) *J. Mol. Biol.* **296,** 295-309
4. Abraham, B. D., Sono, M., Boutaud, O., Shriner, A., Dawson, J. H., Brash, A. R., and Gaffney, B. J. (2001) *Biochemistry* **40,** 2251-2259.
5. Koljak, R., Boutaud, O., Shieh, B. H., Samel, N., and Brash, A. R. (1997) *Science* **277,** 1994-1996.
6. Greer, J. (1971) *J. Mol. Biol.* **59,** 107-126
7. Nagai, K., Kagimoto, T., Hayashi, A., Taketa, F., and Kitagawa, T. (1983) *Biochemistry* **22,** 1305-1311
8. Nagai, M., Yoneyama, Y., and Kitagawa, T. (1989) *Biochemistry* **28,** 2418-2422
9. Pulsinelli, P. D., Perutz, M. F., and Nagel, R. L. (1973) *Proc. Nat. Acad. Sci. U. S. A.* **70,** 3870-3874
10. Adachi, S., Nagano, S., Ishimori, K., Watanabe, Y., Morishima, I., Egawa, T., Kitagawa, T., and Makino, R. (1993) *Biochemistry* **32,** 241-252
11. Egeberg, K. D., Springer, B. A., Martinis, S. A., Sligar, S. G., Morikis, D., and Champion, P. M. (1990) *Biochemistry* **29,** 9783-9791
12. Hildebrand, D. P., Burk, D. L., Maurus, R., Ferrer, J. C., Brayer, G. D., and Mauk, A. G. (1995) *Biochemistry* **34,** 1997-2005
13. Maurus, R., Bogumil, R., Luo, Y. G., Tang, H. L., Smith, M., Mauk, A. G., and Brayer, G. D. (1994) *J. Biol. Chem.* **269,** 12606-12610
14. Pin, S., Alpert, B., Cortes, R., Ascone, I., Chiu, M. L., and Sligar, S. G. (1994) *Biochemistry* **33,** 11618-11623
15. Tang, H. L., Chance, B., Mauk, A. G., Powers, L. S., Reddy, K. S., and Smith, M.

(1994) *Biochim Biophys Acta* **1206,** 90-96

16. Liu, Y., Moenne-Loccoz, P., Hildebrand, D. P., Wilks, A., Loehr, T. M., Mauk, A. G., and de Montellano, P. R. O. (1999) *Biochemistry* **38,** 3733-3743
17. Barrick, D. (1994) *Biochemistry* **33,** 6546-6554
18. Decatur, S. M., Franzen, S., DePillis, G. D., Dyer, R. B., Woodruff, W. H., and Boxer, S. G. (1996) *Biochemistry* **35,** 4939-4944
19. Decatur, S. M., DePillis, G. D., and Boxer, S. G. (1996) *Biochemistry* **35,** 3925-3932
20. Depillis, G. D., Decatur, S. M., Barrick, D., and Boxer, S. G. (1994) *J. Am. Chem. Soc.* **116,** 6981-6982
21. Roach, M. P., Puspita, W. J., and Watanabe, Y. (2000) *J. Inorg. Biochem.* **81,** 173-182
22. Roach, M. P., Ozaki, S., and Watanabe, Y. (2000) *Biochemistry* **39,** 1446-1454
23. Samejima, T., and Yang, J. T. (1963) *J. Biol. Chem.* **238,** 3256-3261
24. Springer, B. A., Egeberg, K. D., Sligar, S. G., Rohlfs, R. J., Mathews, A. J., and Olson, J. S. (1989) *J. Biol. Chem.* **264,** 3057-3060
25. Springer, B. A., and Sligar, S. G. (1987) *Proc. Natl. Acad. Sci. U. S. A.* **84,** 8961-8965
26. Stryer, L. (1988) *Biochemistry*, Freeman, New York
27. Matsui, T., Ozaki, S., Liong, E., Phillips, G. N., and Watanabe, Y. (1999) *J. Biol. Chem.* **274,** 2838-2844
28. Gaber, B. P., Miskowski, V., and Spiro, T. G. (1974) *J. Am. Chem. Soc.* **96,** 6868-6873
29. Que, L., Jr. (1988) in *in Biological Applications of Raman Spectroscopy* (Spiro, T. G., ed) Vol. 3, pp. 491, Wiley, New York
30. Uno, T., Hatano, K., Nishimura, Y., and Arata, Y. (1990) *Inorg. Chem.* **29,** 2803-2807
31. Spiro, T. G. (1983) in *in Iron Porphyrins* (Lever, A. B. P., & Gray, H. B., ed) Vol. 2, pp. 89-159, Addison-Wiley, Reading, MA
32. Chuang, W. J., Johnson, S., and Vanwart, H. E. (1988) *J. Inorg. Biochem.* **34,** 201-

219

33. Sharma, K. D., Andersson, L. A., Loehr, T. M., Terner, J., and Goff, H. M. (1989) *J. Biol. Chem.* **264,** 12772-12779

34. Torii, K., and Ogura, Y. (1969) *J. Biol. Chem.* **65,** 825-827

35. King, N. K., and Winfield, M. E. (1963) *J. Biol. Chem.* **238,** 1520-1528

36. King, N. K., Looney, F. D., and Winfield, M. E. (1964) *Biochim. Biophys. Acta* **88,** 235-236

37. Yonetani, T., and Schleyer, H. (1967) *J. Biol. Chem.* **242,** 1974-1979

38. Puett, J. (1973) *J. Biol. Chem.* **258,** 4623-4634

39. Sage, J. T., Morikis, D., and Champion, P. M. (1991) *Biochemistry* **30,** 1227-1237

40. Blum, H., Chance, B., and Litchfield, W. J. (1978) *Biochim. Biophys. Acta* **534,** 317-321

PART IV

SUMMARY AND CONCLUSION

In the present thesis, the author has aimed to elucidate structure-function relationship for heme enzymes. Sperm whale myoglobin (Mb) has been employed as a building block to reconstruct essential elements of heme enzyme into Mb for his purpose, and some Mb mutants have been prepared by site-directed mutagenesis.

Part II described roles of an electron-rich tryptophan residue in the heme active site. F43W and F43W/H64L Mb were allowed us to examine the effects of an electron-rich tryptophan residue on the catalysis, described in chapter 1. In terms of regulation of substrate binding in the heme enzyme active site, Trp-43 in the mutant appears to be a good model to examine the P-450 type hydroxylation of aromatic molecules because aromatic carbon atoms of tryptophan were fixed in the heme vicinity. Chapter 2 described the oxidative modification of Trp-43 in the heme vicinity of the F43W/H64L Mb.

The replacement of Phe-43 with a tryptophan residue enhances one- and two-electron oxidation activities (i.e. F43W Mb > Wild type Mb and F43W/H64L Mb > H64L Mb). Our results support the hypothesis that an electron-rich oxidizable residue at position 43 would improve the catalytic activity. The improved peroxidase activity (i.e. one-electron process) is due to the acceleration in compound I formation. The enhanced peroxygenase activity (i.e. two-electron process) might be explained by the increase in the reactivity of compound I. However, the rationalization remains to be proved because the oxidative modification of F43W/H64L Mb in compound I formation with *m*CPBA prevents us from determining the actual reactivity of the catalytic species for the intact protein. Finally, the combinations of FPLC and MS analysis allow us to identify that Trp-43 gains a mass by 30 Da due to the post-translational modification.

The indole substructure of Trp-43 in F43W/H64L Mb is oxidatively transformed into 2,6-dihydro-2,6-dioxoindole in the presence of *m*CPBA. Our finding is the first example of the oxidation of aromatic carbons by the myoglobin mutant system as far as we know. The results implicate that a ferryl oxygen atom transfer to aromatic molecules would be possible by a heme enzyme with a non-thiolate ligand if the substrates were fixed nearby the heme iron. In addition, a unique amino-oxo exchange reaction of the amino-terminal 2,6-dihydro-2,6-

dioxoindole performed by Lys-C and trypsin was also reported.

Part III described effects of a phenolate axial ligand on the heme environmental structure. H64Y/H93G and H64Y/H93G/H97L Mb mutants were prepared to construct 5-coordinate ferric high spin heme with a stable tyrosinate coordination.

The double mutation of distal His-64 →Tyr and proximal His-93 → Gly achieve successful conversion of Mb into catalase like protein in terms of coordination structure and electronic properties of ferric heme iron. Regrettably, H64Y/H93G Mb is not react with H_2O_2, while His-93 → Gly mutation gives enough vacant site to accommodate exogenous substrate. Therefore, we conclude that another factor should be required to construct functional model for catalase.

Throughout the work in part II, the oxidative modification of Trp-43 indicates a ferryl oxygen atom transfer to aromatic molecules would be possible by a heme enzyme with a non-thiolate ligand if the substrates were fixed nearby the heme iron. The studies in part III, the double mutation of distal His-64 →Tyr and proximal His-93 → Gly achieve successful conversion of Mb into catalase like protein in terms of coordination structure and electronic properties of ferric heme iron.

ACKOWLEDGMENT

The present thesis is a summary of the author's studies from 1998 to 2001 at Department of Structural Molecular Science, the Graduate University for Advanced Studies. This work is generously supported by Institute for Molecular Science and carried out under supervision of Prof. Yoshihito Watanabe. The author wishes to express his cordial gratitude to Prof. Yoshihito Watanabe for his continual direction, stimulating discussion, and hearty encouragement. The author also owes his accomplishment of the studies to the discerning advice and helpful discussion by associate professor Shin-ichi Ozaki in Yamagata University, research associate Toshitaka Matsui in Tohoku University, research associate Takahumi Ueno in Center for Integrative Bioscience and research associate Seiji Ogo in Institute for Molecular Science.

The author really grateful to Prof. Norikazu Ueyama and Dr. Keonil Lee in Osaka University for NMR measurements of low concentration samples, Prof. Shinobu Itoh in Osaka City University for fruitful discussion about oxidation mechanism of indole derivatives, and associate professor Hiroshi Fujii in Institute for Molecular Science gifts ^{18}O-labeled *m*CPBA to us. The author really grateful to Prof. Teizo Kitagawa in Center for Integrative Bioscience and miss Nami Haruta in The Graduate University for Advanced Studies for resonance Raman measurements about the study in PART III.

This work would not have been possible without help of the members and co-workers in Prof. Watanabe's laboratory. Acknowledgments are also due to Mrs. Misako Tanizawa and Mrs. Akiyo Ota for their office work and heartfelt kindness.

Finally, the author expresses his sincere gratitude to his parents for their supports, generous understanding, and affectionate encouragement.

Okazaki, August 2001

Isao Hara

LIST OF PUBLICATIONS

1. Oxidative Modification of Tryptophan-43 in the Heme Vicinity of the F43W/H64L Myoglobin Mutant
   Isao Hara, Takafumi Ueno, Shin-ichi Ozaki, Shinobu Itoh, Keonil Lee, Norikazu Ueyama, and Yoshihito Watanabe
   J. Biol. Chem. **2001**, *276*, 36067-36070.

2. Molecular Engineering of Myoglobin: The Improvement of Oxidation Activity by Replacing Phe-43 with Tryptophan
   Shin-ichi Ozaki, Isao Hara, Toshitaka Matsui, and Yoshihito Watanabe
   Biochemistry, **2001**, *40*, *4*, 1044-1052.

OTHER PUBLICATIONS

1. Effects of the Arrangement of a Distal Catalytic Residue on Regioselectivity and Reactivity in the Coupled Oxidation of Sperm Whale Myoglobin Mutants
   Tatsuya Murakami, Isao Morishima, Toshitaka Matsui, Shin-ichi Ozaki, Isao Hara, Hui-Jun Yang, and Yoshihito Watanabe
   J. Am. Chem. Soc. **1999**, *121*, 2007-2011.

2. Isolation and characterization of vanadium bromoperoxidase from a marine macroalga, *Ecklonia stolonifera*
   Isao Hara and Takeshi Sakurai
   J. Inorg. Biochem. **1998**, *72*, 23-28.